に，学会などを通じた開発体制の整備が重要と思われる．

おわりに

最近のimmune checkpoint antibodiesの登場により，抗腫瘍薬剤の開発の世界は大きな変革期を迎えている．すなわち，それまで免疫に見向きもしないばかりか，ともすれば批判的であった腫瘍内科医が，免疫治療に目を向けはじめた．そのことは，GCPを準拠した免疫治療臨床開発の質の向上の必要性が叫ばれる今，喜ばしいことではある．一方，免疫モニタリングなどの免疫治療の開発を支える基盤は確立されておらず，今後も基礎研究者の関与は必要である．

文献

1）Topalian, S. L. et al.：N. Engl. J. Med., 366：2443-2454, 2012
2）Brahmer, J. R. et al.：N. Engl. J. Med., 366：2455-2465, 2012
3）Wolchok, J. D. et al.：Clin. Cancer Res., 15：7412-7420, 2009
4）「BBC News：Six taken ill after drug trials」(http://news.bbc.co.uk/2/hi/uk_news/england/london/4807042.stm)
5）Grupp, S. A. et al.：N. Engl. J. Med., 368：1509-1518, 2013

<著者プロフィール>
平家勇司：徳島大学病院，がん研究会がん化学療法センターを経て，1992年より国立がんセンター研究所薬効試験部にてがん化学療法，免疫治療，遺伝子治療の開発研究に従事する．米国アラバマ大学遺伝子治療センターにて，アデノウイルスベクターを用いた遺伝子治療開発に従事した後，'98年より，国立病院四国がんセンター内科・臨床研究部にて，診療ならびに臨床研究に従事．2002年より国立がんセンターにて，造血幹細胞移植，免疫療法，遺伝子治療の臨床開発に従事する．

特集　変貌するがん免疫療法

細胞免疫療法の現状と展望*

平家勇司**

Key Words：dendritic cell, TCR-T, CAR-T

はじめに

細胞免疫療法は，Steven Rosenberg博士が悪性黒色種に対するLAK療法の治療有用性を示唆する報告をして以来[1]，腫瘍内浸潤リンパ球療法，CTL療法，樹状細胞療法と，その時代の基礎免疫の研究成果を取り入れ開発が試みられてきた．しかし，現時点では，その有効性が認められ承認されたものは，Dendreon社の前立腺がんに対する樹状細胞(sipuleucel-T)のみである．

現在，がんに対する免疫療法が注目を集めているが，その主流は抗PD-1抗体や抗CTLA-4抗体に代表される免疫制御抗体である[2)~5)]．免疫制御抗体は，今までの化学療法剤でみられない強い腫瘍制御能を示唆するデータが得られており，当面，免疫療法の世界では免疫制御抗体を用いた治療開発が主流になるのは疑いない．一方，免疫制御抗体は，強い肝障害や，自己免疫疾患をひき起こすことが明らかとなっており，その適応に関しては今後も検討が必要と考える．

免疫制御抗体とともに，現在注目を集めている新たな免疫治療として，遺伝子改変T細胞療法がある．これには，T細胞受容体(T cell receptor；TCR)遺伝子を導入したTCR-T細胞療法と，chimeric-artificial-receptor(CAR)遺伝子を導入した，CAR-T細胞療法がある．

本総説では，米国で承認されている前立腺がんに対する樹状細胞療法に加え，現在注目を集めているこの2つの遺伝子改変T細胞療法を紹介する．

樹状細胞療法

樹状細胞療法とは，抗原特異的なリンパ球を誘導，増殖活性化させる司令塔の役割を担っている樹状細胞を，体外で増殖，抗原刺激を行い活性化した上で，患者に戻す方法である．投与された樹状細胞は，患者体内で抗原特異的リンパ球を増殖・活性化し，抗腫瘍効果を誘導する．

Sipuleucel-T(Provenge®)とは，自己末梢血単核球をGM-CSFと腫瘍抗原prostatic acid phosphatase(PAP)の融合蛋白で刺激して製造した自己由来樹状細胞である．Sipuleucel-Tの臨床第III相試験には，ホルモン療法耐性の前立腺がん患者512名が登録され，うち341名がsipuleucel-Tの投与を，171名がplaceboの投与を受けた．その結果，sipuleucel-T投与群がPlacebo群より4.1か月の延命効果が得られ，2010年にFood and Drug Administration(FDA)により承認された(図1)[6]．Sipuleucel-Tは，International Conference for Harmonization(ICH)参加国の中で最初に承認された細胞療法として注目を集めた．一方で，この治療にかかる費用は9万3,000ドルと高額であ

* Current status and future prospects of cellular immunotherapy.

** Yuji HEIKE, M.D., Ph.D.: 独立行政法人国立がん研究センター早期・探索臨床研究センター免疫療法開発分野〔〒104-0045 東京都中央区築地5-1-1〕; Division of Cancer Immunotherapy, Exploratory Oncology Research & Clinical Trial Center, National Cancer Center, Tokyo 104-0045, JAPAN

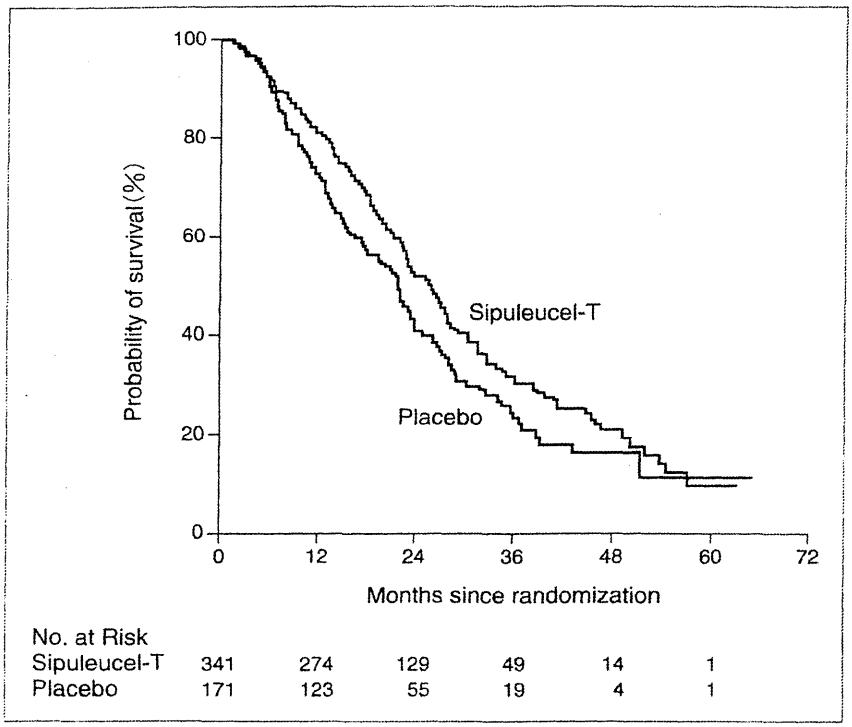

図1　Sipuleucel-Tによる，ホルモン療法耐性の前立腺がん患者の生存率の延長効果
Sipuleucel-T投与群の生存期間中央値が25.8か月であるのに対し，placebo群の生存期間中央値は21.7か月であった．36か月時点の生存率は，sipuleucel-T投与群が31.7％であるのに対し，placeboは23.0％であった．（文献[6]より引用）

り，効果/費用比に関してはいまだに議論が続いており，どこまで普及するかは，現時点では不透明である．

わが国においても，いくつかの大学，先端的医療機関やバイオベンチャーが，自主研究，先進医療あるいは自由診療のかたちで樹状細胞療法の臨床研究，実地診療を行っている．そのなかには，human leukocyte antigen（HLA）拘束性の抗原ペプチドをパルスした樹状細胞に加え，抗原蛋白やそのmRNAを導入したHLA非拘束性の樹状細胞など，より進化した手法を用いているものある．しかし，いずれも非Good Clinical Practice（GCP）下での臨床研究であり，承認に直結する試験とはなっていない．今後，GCPに準拠した試験を行い，その安全性と有効性を検証することが必要と考える[7)~9)]．

リンパ球療法

「はじめに」にも記載したように，最初に注目を集めた細胞免疫療法は，1988年にNational Institutes of Health（NIH）のRosenberg博士が報告した活性化リンパ球（LAK）療法である．その後，腫瘍内浸潤リンパ球療法，抗原特異的リンパ球療法，γδT細胞療法等，さまざまなリンパ球療法が試みられてきたが，国内外を含め，承認に結びついているものはない．近年，バイオテクノロジーの進歩によって，抗原特異的なTCRのクローニングとリンパ球での遺伝子発現，さらにはCAR遺伝子の構築とその発現が可能となり，腫瘍特異性と抗腫瘍活性を飛躍的に高めた遺伝子導入リンパ球療法が開発され，注目を集めている．

1．TCR遺伝子導入Tリンパ球（TCR-T）療法

腫瘍細胞上のHLA-抗原ペプチド複合体を認識するリンパ球クローンから，抗原特異的TCR遺伝子をクローニングし，発現ベクターを構築した上で患者リンパ球に導入，大量培養した上で患者に投与する方法である．TCR-T療法は，HLA拘束性があり対象患者が絞られてしまうものの，一方では腫瘍の増殖にかかわる核内蛋白等，細

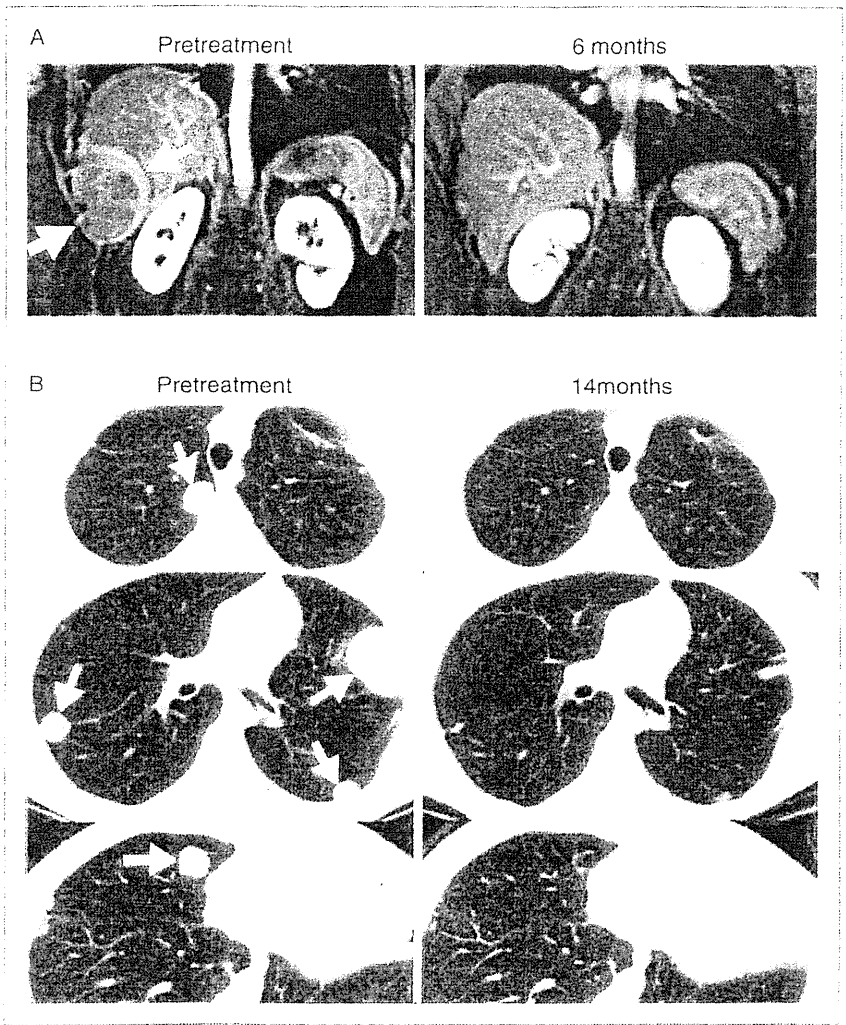

図２　滑膜肉腫に対するNY-ESO-1 TCR-Tの治療効果
A：胸壁（肝周囲領域）腫瘤 治療後６か月時点でpartial response（PR），B：肺転移 治療後14か月時点でPR　（文献[10]より引用）

胞膜表面に発現していない蛋白も標的とすることが可能である．現在までに，欧米人に多いHLA-A0201を持つ患者を対象に，NY-ESO-1[10]，MAGE-A3[11,12]，WT-1[13]等に対するTCR遺伝子導入リンパ球の試験が行われ，その成果が報告されている．わが国においてもHLA-A2402拘束性MAGE-A4やWT1特異的TCR遺伝子導入リンパ球の研究者主体の自主研究ならびに治験が実施，準備されている．

TCR-Tの臨床応用においては，米国National Cancer Institute（NCI）のRosenberg博士のグループが複数の報告を行っている．HLA-A0201を有するNY-ESO-1陽性進行滑膜肉腫患者ならびに進行悪性黒色腫患者を対象とした，NY-ESO-1 TCR-T細胞療法では，TCR-Tが投与された６名の滑膜肉腫の患者のうち４例，悪性黒色腫患者11例中５例で明らかな腫瘍の縮小がみられ，うち２名の悪性黒色腫患者は完全寛解状態が１年以上継続したことが報告されている（図２）[10]．MAGE-A3 TCR-Tの臨床試験では，９例の進行がん患者が登録された．うち５例で腫瘍の縮小効果がみられたものの，３例においてMAGE-A3 TCR-T投与後２以内に精神障害が出現し，うち２例が昏睡状態になり死亡した．MRIを用いた画像解析で脳室周囲の白質軟化症が認められ，さらに病理解析の結果，その領域にCD8陽性Ｔ細胞の浸潤

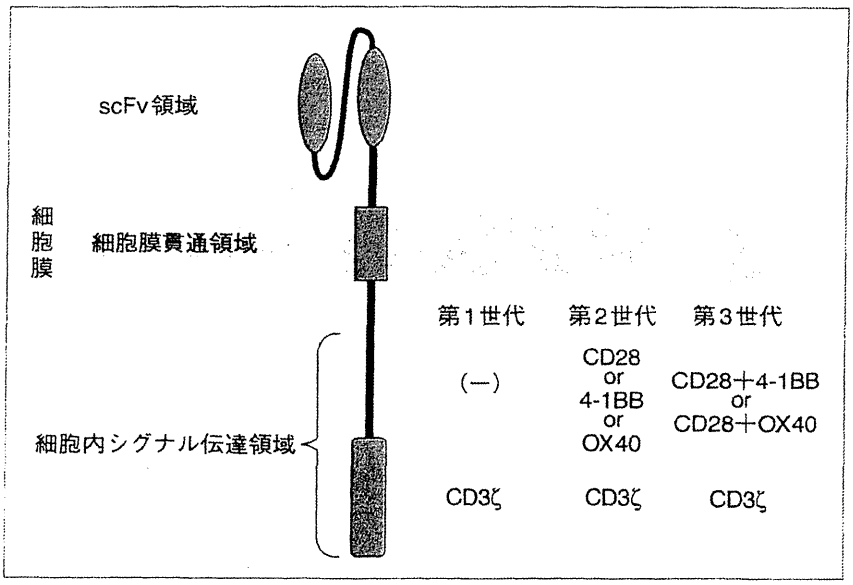

図3　Chimeric-artificial-receptor(CAR)の構造
CARは，抗原を認識するscFv領域，細胞膜貫通領域と細胞内シグナル伝達領域で構成される．第1世代のCARは，細胞内シグナル伝達領域のCD3ζのみを使用していたが，抗腫瘍効果は弱かった．第2世代CARは，副刺激分子(CD28, 4-1BB, OX-40等)由来のシグナル伝達領域を融合させることで，殺細胞効果が格段に高まった．

を伴っていることが明らかとなった．Real time PCRを用いた詳細な解析の結果，脳内正常脳細胞において，通常の解析では検出できないレベルのMAGE-A12等MAGE familyの発現が認められ，投与したMAGE-A3 TCR-TがこれらMAGE family由来の抗原に対し免疫反応を起こした可能性が高いことが明らかとなった[11)12)]．この事実は，TCR-Tの有害事象を予測するには，免疫染色等の一般的な検査では不十分である可能性を示唆しており，開発を行う研究者にとって衝撃的であった．今後は，TCR-T療法において予測できない有害事象が起こりうることを前提に，注意深い観察をしながら臨床応用を進めていくことが求められる．

TCRはα鎖とβ鎖のヘテロダイマーで構成されている．そのため，TCR遺伝子導入T細胞の中で，導入したα鎖，β鎖と内在性のα鎖，β鎖が交互に結合し，結果として4種類のTCRが出現する．その結果，標的抗原を持つ細胞に対する殺細胞効果が弱まったり，目的以外の抗原に反応し有害事象につながる可能性が拭い去れない．そこで，short interfering RNA(siRNA)の手法を用いて内在性TCRを発現抑制し，導入したTCRのみが発現するよう工夫したベクターが開発されている[14)]．

このように，TCR-Tは，魅力的な治療法ではあるものの，現時点では予想できない有害事象が出現することも想定し，最先端の技術を用いて安全性を高める努力を行うとともに，臨床開発は慎重に進めることが重要と考える．

2. Chimeric-antigen-receptor遺伝子導入Tリンパ球(CAR-T)療法

TCR-T療法にもまして注目を集めているのは，CAR-T療法である．CARとは，細胞膜表面の抗原を認識する抗体のscFvと，細胞膜貫通領域，細胞内シグナル伝達領域の3つの部分から構成される融合蛋白である．この融合蛋白をT細胞に遺伝子導入し発現させたものがCAR-Tであり，scFvが認識する抗原発現細胞を認識，破壊する．当初，CD3由来のCD3ζのみをシグナル伝達部位として用いたCARが作られたが，十分な抗腫瘍効果が得られなかった．そこで，CD3ζにCD28や4-1BBのシグナル伝達領域を融合させた，より高い抗腫瘍活性を持つ第2世代のCARが構築され，

臨床試験で用いられている[15)~17)](図3)．現在，CAR-Tの中でも，CD19分子を標的とするCAR-T(CD19CAR-T)の早期臨床開発の結果が，血液内科医の注目を集めている．Pennsylvania大学のCarl June博士は，acute lymphocytic leukemia(ALL)とchronic lymphocytic leukemia(CLL)に対するCD19CAR-Tの臨床応用の症例報告をそれぞれN Engl J Medに[18)19)]，Memorial Sloan Kettering Cancer Center(MSKCC)のRenier J. BrentjensらはALLに対する治療的有用性をSci Transl Medに報告した[20)]．これらの報告は，全体としての有効性を議論するには症例数が少ないが，既存の化学療法で完全寛解に達しない症例が寛解となり，長期間維持されているのは注目に値する．一方，この報告の中で，サイトカインストーム，腫瘍崩壊症候群，マクロファージ活性化症候群(IL-6, IFN-γが関与)等，致死的あるいはquality of life(QOL)を著しく低下させる有害事象が出現することも報告している．さらに，投与したCD19CAR-Tは体内に長期間にわたって存在し，正常B細胞の回復をも阻害し，無γ-globulin血漿をひき起こす．

CD19CAR-T投与に伴うサイトカインストームは，抗サイトカイン抗体療法での対応が可能であるが，長期に及ぶ無γ-globulin血漿は補充療法以外の対処方法がないことから，大きな問題となると思われる．特に予後が長く，成長期を控えている小児患者に対し，対応が必要と考える．

現在，複数の施設で遺伝子構成やベクターが異なるCD19CAR-Tの臨床開発が並行して行われている[15)]．すでに，Pennsylvania大学の抗CD19CAR-T細胞の開発権はNovartisが獲得し，global治験実施に向けた準備を進めている．わが国においても，自治医科大学の小澤教授のグループが，タカラバイオと協力してMSKCCのベクターを用いた臨床試験を準備している．一方，米国では，異なるCD19CAR-Tの開発を行っている研究者同士でベクターを相互に供給し，ベクター間での有効性・安全性を比較検討するNCI STRAP Studyも計画されており，その結果が注目されている．

CD19以外にも，複数の抗原に対するCAR遺伝子導入T細胞が作られ，臨床応用が試みられおり，これらの臨床結果にも注目が集まっている[17)]．

おわりに

1988年に，Rosenberg博士がLAK療法の有用性を報告してから四半世紀が経とうとしている．その間，数々の細胞療法が現れては消え，現時点で承認が得られいてるのはDendreon社の前立腺がんに対する樹状細胞療法のみである．そのようななか，抗CTLA-4抗体や抗PD-1抗体に代表される免疫制御抗体の有用性が証明され，腫瘍内科医の中では，「がん免疫療法＝免疫制御抗体」のイメージが定着しつつある．一方で，免疫制御抗体は肝障害や自己免疫疾患を誘導するなど，重篤な有害事象も避けて通れない．細胞免疫療法は，免疫制御抗体の対象とならない患者，あるいは併用療法として，新たな治療手技となる可能性を秘めている．

今，日本はiPSがきっかけとなり，細胞療法の臨床開発を促進する機運に包まれている．このなかで，アカデミア，企業さらには規制当局者が協力して，しっかりとした細胞免疫療法開発基盤を構築し，国内外のオンコロジストからも評価される細胞免疫療法を確立していくことが重要である．

文　献

1) Rosenberg SA, Lotze MT, Muul LM, et al. A progress report on the treatment of 157 patients with advanced cancer using lymphokine-activated killer cells and interleukin-2 or high-dose interleukin-2 alone. N Engl J Med 1987 ; 316 : 889.
2) Hodi FS, O'Day SJ, McDermott DF, et al. Improved survival with ipilimumab in patients with metastatic melanoma. N Engl J Med 2010 ; 363 : 711.
3) Topalian SL, Hodi FS, Brahmer JR, et al. Safety, activity, and immune correlates of anti-PD-1 antibody in cancer. N Engl J Med 2012 ; 366 : 2443.
4) Brahmer JR, Tykodi SS, Chow LQ, et al. Safety and activity of anti-PD-L1 antibody in patients with advanced cancer. N Engl J Med 2012 ; 366 : 2455.
5) Pardoll DM. The blockade of immune checkpoints in cancer immunotherapy. Nat Rev Cancer 2012 ; 12 : 252.
6) Kantoff PW, Higano CS, Shore ND, et al. Sipuleucel-

T immunotherapy for castration-resistant prostate cancer. N Engl J Med 2010 ; 363 : 411.

7) Akiyama, Y, Oshita C, Kume A, et al. Alpha-type-1 polarized dendritic cell-based vaccination in recurrent high-grade glioma : a phase I clinical trial. BMC Cancer 2012 : 12, 623.

8) Oshita C, Takikawa M, Kume A, et al. Dendritic cell-based vaccination in metastatic melanoma patients : phase II clinical trial. Oncol Rep 2012 ; 28 : 1131.

9) Kimura Y, Tsukada J, Tomoda T, et al. Clinical and immunologic evaluation of dendritic cell-based immunotherapy in combination with gemcitabine and/or S-1 in patients with advanced pancreatic carcinoma. Pancreas 2012 ; 41 : 195.

10) Robbins PF, Morgan RA, Feldman SA, et al. Tumor regression in patients with metastatic synovial cell sarcoma and melanoma using genetically engineered lymphocytes reactive with NY-ESO-1. J Clin Oncol 2011 ; 29 : 917.

11) Brichard VG, Louahed J, Clay TM. Cancer regression and neurological toxicity cases after anti-MAGE-A3 TCR gene therapy. J Immunother 2013 ; 36 : 79.

12) Morgan RA, Chinnasamy N, Abate-Daga D, et al. Cancer regression and neurological toxicity following anti-MAGE-A3 TCR gene therapy. J Immunother 2013 ; 36 : 133.

13) WT1 TCR Gene Therapy for Leukemia : A Phase I/II Safety and Toxicity Study (WT1 TCR-001). Available from : URL : http://clinicaltrials.gov/show/NCT01621724.

14) Ochi T, Fujiwara H, Okamoto S, et al. Novel adoptive T-cell immunotherapy using a WT1-specific TCR vector encoding silencers for endogenous TCRs shows marked antileukemia reactivity and safety. Blood 2011 ; 118 : 1495.

15) Lipowska-Bhalla G, Gilham DE, Hawkins RE, et al. Targeted immunotherapy of cancer with CAR T cells : achievements and challenges. Cancer Immunol Immunother 2012 ; 61 : 953.

16) Gilham DE, Debets R, Pule M, et al. CAR-T cells and solid tumors : tuning T cells to challenge an inveterate foe. Trends Mol Med 2012 ; 18 : 377.

17) Kohn DB, Dotti G, Brentjens R, et al. CARs on track in the clinic. Mol Ther 2011 ; 19 : 432.

18) Grupp SA, Kalos M, Barrett D, et al. Chimeric antigen receptor-modified T cells for acute lymphoid leukemia. N Engl J Med 2013 ; 368 : 1509.

19) Porter DL, Levine BL, Kalos M, et al. Chimeric antigen receptor-modified T cells in chronic lymphoid leukemia. N Engl J Med 2011 ; 365 : 725.

20) Brentjens RJ, Davila ML, Riviere I, et al. CD19-targeted T cells rapidly induce molecular remissions in adults with chemotherapy-refractory acute lymphoblastic leukemia. Sci Transl Med 2013 ; 5 : 177ra38.

* * *

Gene Therapy (2013) **20,** 112 - 118

www.nature.com/gt

SHORT COMMUNICATION

A simple detection system for adenovirus receptor expression using a telomerase-specific replication-competent adenovirus

T Sasaki[1], H Tazawa[2,3], J Hasei[1], S Osaki [1], T Kunisada[1,4], A Yoshida[1], Y Hashimoto[3], S Yano[3], R Yoshida[3], S Kagawa[3], F Uno[3], Y Urata[5], T Ozaki[1] and T Fujiwara[3]

Adenovirus serotype 5 (Ad5) is frequently used as an effective vector for induction of therapeutic transgenes in cancer gene therapy or of tumor cell lysis in oncolytic virotherapy. Ad5 can infect target cells through binding with the coxsackie and adenovirus receptor (CAR). Thus, the infectious ability of Ad5-based vectors depends on the CAR expression level in target cells. There are conventional methods to evaluate the CAR expression level in human target cells, including flow cytometry, western blotting and immunohistochemistry. Here, we show a simple system for detection and assessment of functional CAR expression in human tumor cells, using the green fluorescent protein (GFP)-expressing telomerase-specific replication-competent adenovirus OBP-401. OBP-401 infection induced detectable GFP expression in CAR-expressing tumor cells, but not in CAR-negative tumor cells, nor in CAR-positive normal fibroblasts, 24 h after infection. OBP-401-mediated GFP expression was significantly associated with CAR expression in tumor cells. OBP-401 infection detected tumor cells with low CAR expression more efficiently than conventional methods. OBP-401 also distinguished CAR-positive tumor tissues from CAR-negative tumor and normal tissues in biopsy samples. These results suggest that GFP-expressing telomerase-specific replication-competent adenovirus is a very potent diagnostic tool for assessment of functional CAR expression in tumor cells for Ad5-based antitumor therapy.

Gene Therapy (2013) **20,** 112–118; doi:10.1038/gt.2011.213; published online 12 January 2012

Keywords: oncolytic virus; adenovirus; telomerase; sarcoma; GFP

INTRODUCTION

Adenovirus serotype 5 (Ad5) is widely and frequently used as an effective vector in cancer gene therapy and oncolytic virotherapy.[1-3] Adenovirus-mediated transgene transduction is a highly efficient method for induction of ectopic transgene expression in tumor cells.[1,2] The p53 tumor suppressor gene, which is a potential therapeutic transgene that may induce a very strong antitumor effect, has been transduced into tumor cells using a replication-deficient adenovirus vector (Ad-p53, Advexin, Intorgen Therapeutics, Inc., Austin, TX, USA), and Ad-p53 has been reported to induce an antitumor effect in clinical studies.[4-7] Recently, an Ad5-based replication-competent oncolytic adenovirus has been developed as a promising anticancer reagent for induction of tumor-specific cell lysis.[8,9] Ad5-based vectors infect human target cells through binding with the coxsackie and adenovirus receptor (CAR).[10] Thus, the infection efficiency of Ad5-based vectors mainly depends on the CAR expression level in tumor tissues.[11-17] Increased CAR expression has been frequently shown in tumor cells in various organs such as the brain,[18] thyroid,[19] esophagus,[20] gastrointestinal tract,[21] prostate,[14] bone and soft tissues.[22-24] However, tumor cells often show reduced CAR expression following tumor progression.[18,21,25,26] Decreased CAR expression has also been shown in tumor tissues after repeated injection of Ad-p53.[27,28] It is therefore necessary to assess the CAR expression level of target tumor tissues before and after Ad5-based cancer gene therapy and oncolytic virotherapy.

There are some conventional methods for evaluation of the CAR expression level in tumor tissues, such as flow cytometry, immunohistochemistry, western blotting and reverse transcription (RT)-PCR. Flow cytometry is mainly used to detect CAR-positive human tumor cell lines.[13,24,28,29] Immunohistochemistry is frequently used to assess CAR expression in various human tumor tissues.[11,14,20,23,25] Western blotting is usually performed to confirm the expression of many types of proteins including CAR in molecular biological experiments. Quantitative RT-PCR is also a useful method for evaluation of the mRNA expression of CAR.[18,22] Although these conventional methods can detect CAR expression in tumor tissues, it still remains unclear whether Ad5-based vectors really infect target tumor cells through binding with the CAR that is detected using conventional methods. Therefore, the development of a novel method for assessment of the level of expression of functional CAR in tumor tissues, which is what the Ad5-based vectors really bind, is required for Ad5-based anticancer therapy.

We previously developed a telomerase-specific replication-competent adenovirus OBP-301 (Telomelysin, Oncolys BioPharma, Inc., Tokyo, Japan) that drives the *E1A* and *E1B* genes under the human telomerase reverse transcriptase (*hTERT*) promoter.[8,29-31] OBP-301 infects both normal and tumor cells that express CAR, but replicates only in CAR-positive tumor cells in a telomerase-dependent manner. Furthermore, we recently generated a green fluorescent protein (GFP)-expressing telomerase-specific replication-

[1]Department of Orthopaedic Surgery, Okayama University Graduate School of Medicine, Dentistry and Pharmaceutical Sciences, Okayama, Japan; [2]Center for Gene and Cell Therapy, Okayama University Hospital, Okayama, Japan; [3]Department of Gastroenterological Surgery, Okayama University Graduate School of Medicine, Dentistry and Pharmaceutical Sciences, Okayama, Japan; [4]Department of Medical Materials for Musculoskeletal Reconstruction, Okayama University Graduate School of Medicine, Dentistry and Pharmaceutical Sciences, Okayama, Japan and [5]Oncolys BioPharma, Inc., Tokyo, Japan. Correspondence: Professor T Fujiwara, Department of Gastroenterological Surgery, Okayama University Graduate School of Medicine, Dentistry and Pharmaceutical Sciences, 2-5-1 Shikata-cho, Kita-ku, Okayama 700-8558, Japan.
E-mail: toshi_f@md.okayama-u.ac.jp
Received 15 July 2011; revised 7 November 2011; accepted 5 December 2011; published online 12 January 2012

competent adenovirus OBP-401, which induces ectopic GFP expression in tumor cells, but not in normal cells.[32] OBP-401 infection efficiently induces GFP expression in metastatic tumor cells at regional lymph nodes[32] and liver,[33] circulating tumor cells in blood flow[34] and disseminated tumor cells in the abdominal cavity.[35] These results suggest that OBP-401 is a highly sensitive tool for the detection of tumor cells. Furthermore, Ad5-based OBP-401 would also be useful for induction of GFP expression in CAR-positive tumor cells, but not in CAR-negative tumor cells.

In the present study, we evaluated whether induction of GFP expression by OBP-401 infection is associated with CAR expression in tumor cells. OBP-401-mediated GFP induction was further examined in xenograft tumor tissues that have different levels of CAR expression and in surrounding normal tissues.

RESULTS AND DISCUSSION

Assessment of an OBP-401 infection protocol for the detection of CAR-positive tumor cells

We recently demonstrated that the level of CAR expression that was detected using flow cytometry was significantly associated with OBP-301-mediated cytopathic activity in human bone and soft tissue sarcoma cells.[29] Furthermore, OBP-401 infection has been shown to induce GFP expression 24 h after infection of human sarcoma cells.[34] To evaluate whether GFP expression that is induced by OBP-401 infection is associated with CAR expression in tumor cells, we used three human sarcoma cell lines (OST, NMFH-1 and OUMS-27) that have different levels of CAR expression, as previously reported.[29] Flow cytometric analysis confirmed that OST cells showed detectable CAR expression, whereas cells of the NMFH-1 and OUMS-27 sarcoma cell lines had no detectable CAR expression (Figure 1a).

To determine suitable conditions for OBP-401 infection in order to detect CAR-positive tumor cells, OST sarcoma cells were infected with OBP-401 at multiplicity of infections (MOIs) of 1, 10 and 100 plaque-forming units (PFU) per cell over 24 h (Figure 1b and c). Twelve hours after infection, only OBP-401 infection at an MOI of 100 had induced GFP expression in all of the OST cells. Twenty-four hours after infection, OBP-401 infection at MOIs of 10 and 100 had induced ectopic GFP expression in all of the OST cells, whereas OBP-401 infection at an MOI of 1 had induced GFP expression in about 80% of the OST cells. These results indicate that OBP-401 infection at an MOI of greater than 10 is necessary to efficiently detect CAR-positive tumor cells 24 h after infection.

To subsequently determine a suitable condition for OBP-401 infection that would exclude CAR-negative tumor cells, the NMFH-1 and OUMS-27 sarcoma cells that do not express CAR were infected with OBP-401 at MOIs of 10 and 100 for 60 h (Figures 1d and e). NMFH-1 cells expressed GFP at 24 and 48 h after OBP-401 infection at MOIs of 100 and 10, respectively. In contrast, OUMS-27 cells exhibited no GFP expression after OBP-401 infection. To investigate the different GFP expression between these CAR-negative tumor cells, expression of integrins, $\alpha v\beta 3$ and $\alpha v\beta 5$, was further examined by flow cytometry. NMFH-1 cells showed twofold higher expression of integrin $\alpha v\beta 3$ compared with OUMS-27 cells, whereas $\alpha v\beta 5$ expression was similar in these cells (Supplementary Figure S1a). These results indicate that OBP-401 infection at an MOI of 10 for 24 h is a suitable protocol for distinguishing CAR-negative tumor cells from CAR-positive tumor cells, when CAR-negative tumor cells express integrin molecules.

Relationship between OBP-401-induced GFP expression and CAR expression

To evaluate whether OBP-401-induced GFP expression correlates with CAR expression in tumor cells, six human sarcoma cell lines (OST, U2OS, NOS-10, MNNG/HOS, NMFH-1 and OUMS-27) and normal human lung fibroblasts (NHLF) cells that have different levels of CAR expression (Figure 1a and Supplementary Figure S1b) were infected with OBP-401 at an MOI of 10 for 24 h, and the GFP-positive cells in each cell type were analyzed under fluorescence microscopy (Figures 2a and b). OBP-401 infection-induced GFP expression from 12 h after infection and, after 24 h, more than 40% of all CAR-positive tumor cells (OST, U2OS, NOS-10 and MNNG/HOS) were detected as GFP-positive cells. However, no GFP-positive cells were detected in the CAR-negative tumor cells (NMFH-1, OUMS-27), or in the normal NHLF cells, 24 h after infection. Furthermore, OBP-401-mediated GFP induction in CAR-positive tumor cells was suppressed by blocking CAR proteins with anti-CAR antibody (Supplementary Figure S2). To assess the GFP expression level in all tumor and normal cells in a more quantitative manner, we quantified the level of GFP fluorescence in each cell type 24 h after infection using a fluorescence microplate reader (Figure 2c). We also quantified the level of CAR expression in these cells by calculating the mean fluorescence intensity in flow cytometric analysis (Figure 2d). GFP fluorescence was detected in CAR-positive tumor cells, but not in either CAR-negative tumor cells or in CAR-positive normal cells. There was a significant relationship between the CAR expression level and the GFP fluorescence level ($r = 0.885$; $P = 0.019$) (Figure 2e). These results indicate that OBP-401-mediated GFP expression is highly associated with CAR expression in tumor cells.

Comparison of the potential of OBP-401-mediated GFP induction and of conventional methods for CAR detection

To estimate the potential of OBP-401-mediated GFP induction for the detection of CAR-positive tumor cells, we compared the above protocol using OBP-401 with western blot analysis and immunocytochemistry. CAR expression was detected in OST, U2OS and NOS-10 sarcoma cells, but not in CAR-positive MNNG/HOS sarcoma cells, using western blot analysis (Supplementary Figure S3a). In contrast, only OST cells displayed a positive CAR signal using immunocytochemistry, whereas the CAR signal of the other three CAR-positive tumor cells was almost as weak as that from CAR-negative tumor cells (Supplementary Figure S3b). CAR expression was also not detected in CAR-positive NHLF cells by either western blot analysis or by immunocytochemistry. These results suggest that the GFP induction protocol using OBP-401 is more sensitive for the detection of CAR-positive tumor cells than conventional methods.

OBP-401-mediated GFP induction was detected in MNNG/HOS sarcoma cells that expressed a low level of CAR (Figure 2c), although neither western blot analysis nor immunocytochemistry detected CAR in these cells (Supplementary Figure S3). Furthermore, although conventional methods may be able to detect high CAR expression in tumor cells, whether the CAR expression that is detected by conventional methods is really functional for binding with Ad5-based vectors still remains unclear. In contrast, as OBP-401 is an Ad5-based vector that expresses a fluorescent *GFP* gene, OBP-401-induced GFP expression directly proves that the CAR that is expressed is functional for Ad5-based vector binding. Thus, the OBP-401-mediated GFP induction strategy is a potential diagnostic method that can efficiently and directly assess functional CAR expression in tumor cells.

OBP-401-mediated GFP induction in xenograft tumor and normal tissues with different CAR expression

Finally, to investigate the potential of the OBP-401-mediated method for the detection of CAR expression in tumor and normal tissues, we used this method to analyze CAR expression of human xenograft tumor tissues, that do or do not express CAR, as well as of surrounding normal muscle tissues, which have been previously shown to lose CAR expression.[36] CAR-positive OST sarcoma cells or CAR-negative OUMS-27 sarcoma cells were inoculated into nude

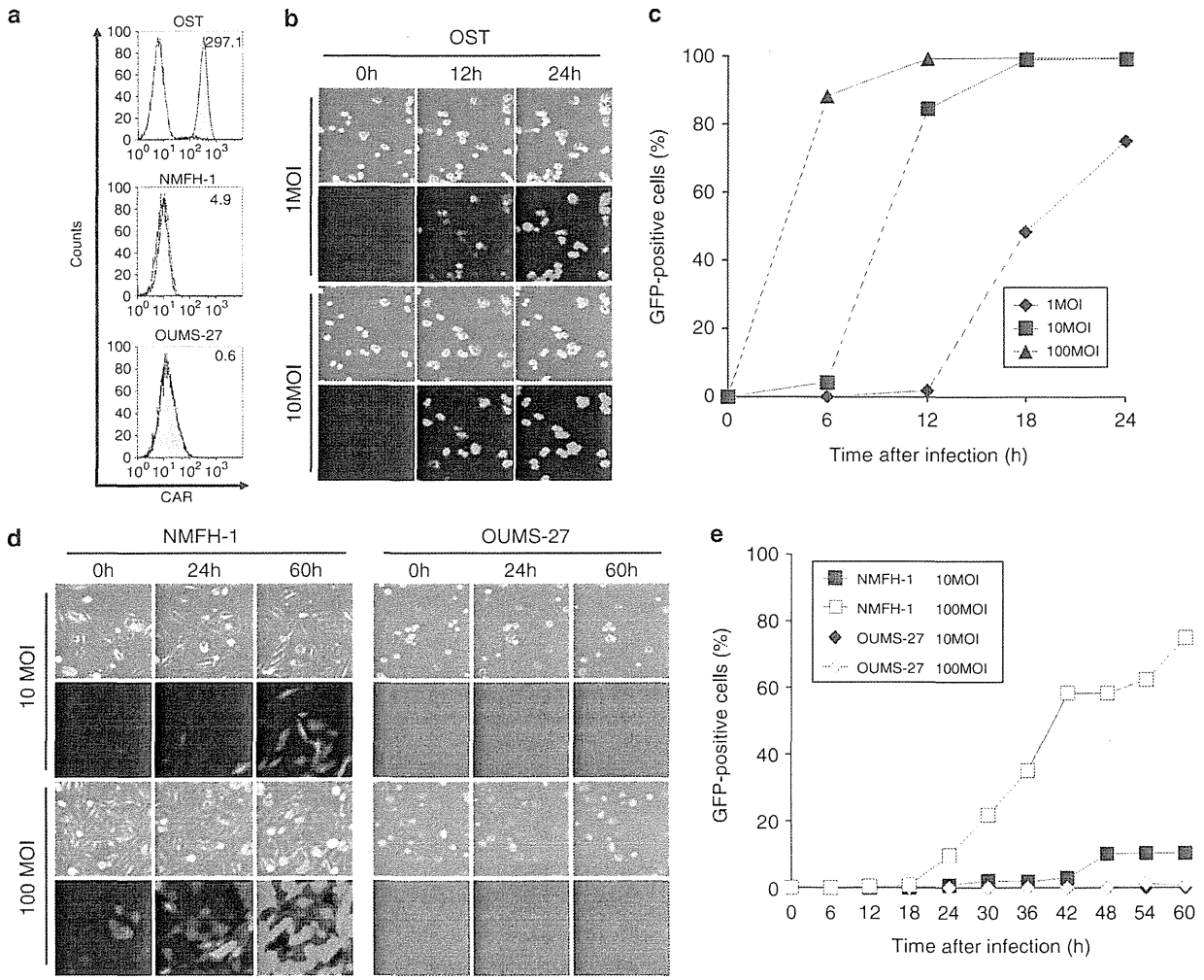

Figure 1. Establishment of a suitable protocol for the detection of CAR expression using OBP-401. (**a**) The level of CAR expression on three human sarcoma cell lines (OST, NMFH-1 and OUMS-27) was analyzed using flow cytometry. The cells were incubated with a monoclonal anti-CAR (RmcB) antibody and the signal was detected using a fluorescent isothiocyanate (FITC)-labeled secondary antibody. The mean fluorescence intensity (MFI), which is a measure of CAR and integrin expression, was calculated for each cell and is shown at the top right of each graph. (**b**) Time-lapse images of OST cells, which displayed the highest CAR expression, were recorded for 24 h after OBP-401 infection at MOIs of 1 and 10 PFU per cell. Representative images taken at the indicated time points and MOIs show cell morphology that was analyzed using phase-contrast microscopy (top panels) and GFP expression that was analyzed using fluorescence microscopy (bottom panels). Original magnification: × 80. (**c**) The percentage of GFP-positive cells was counted in OST cells at the indicated time points after OBP-301 infection at MOIs of 1, 10 and 100 PFU per cell. (**d**) Time-lapse images of non-CAR-expressing OUMS-27 and NMFH-1 cells were recorded for 60 h after OBP-401 infection at MOIs of 10 and 100 PFU per cell. Representative images taken at the indicated time points and MOIs show cell morphology that was analyzed using phase-contrast microscopy (top panels) and GFP expression that was analyzed using fluorescence microscopy (bottom panels). Original magnification: × 80. (**e**) The percentage of OUMS-27 and NMFH-1 GFP-positive cells was counted at the indicated time points after OBP-301 infection at MOIs of 10 and 100 PFU per cell.

mice to develop xenograft tumors. After resection of the OST tumors, the OUMS-27 tumors and normal muscle tissue, the tissues were subjected to the protocol for OBP-401-mediated GFP induction using a three-step procedure (Figure 3a) as follows; step 1: OBP-401 infection for 24 h, step 2: washing with PBS and step 3: observation under a fluorescence microscope. As shown in Figure 3b, OBP-401 infection-induced GFP expression in CAR-positive OST tumor tissues, but not in CAR-negative OUMS-27 tumor tissues or in normal muscle tissue. These results suggest that OBP-401-mediated GFP induction is a simple and useful method for the detection of CAR expression by tumor tissues.

Flow cytometry is a highly sensitive conventional method for the detection of cell surface CAR expression, which is associated with the therapeutic efficacy of Ad5-based vectors in tumor cells.[13,24,28,29] However, as many tumor cells tightly bind to each other or to normal stromal cells within tumor tissues, the preparation of single tumor cells is not easy, and therefore flow cytometry is an inadequate method for the detection of CAR expression in tumor tissues. In contrast, the preparation of single tumor cells is not necessary for the OBP-401-mediated GFP induction protocol. Furthermore, assay of OBP-401-induced GFP expression was more sensitive than flow cytometry (Figure 2d) in distinguishing CAR-positive normal cells from CAR-positive tumor cells (Figure 2c). Thus, the OBP-401-mediated GFP induction method is a simple and tumor-specific system for the detection of CAR expression in tumor tissues.

Fluorescent proteins including GFP have great potentials to visualize tumor cells in real time on the *in vivo* setting.[37,38]

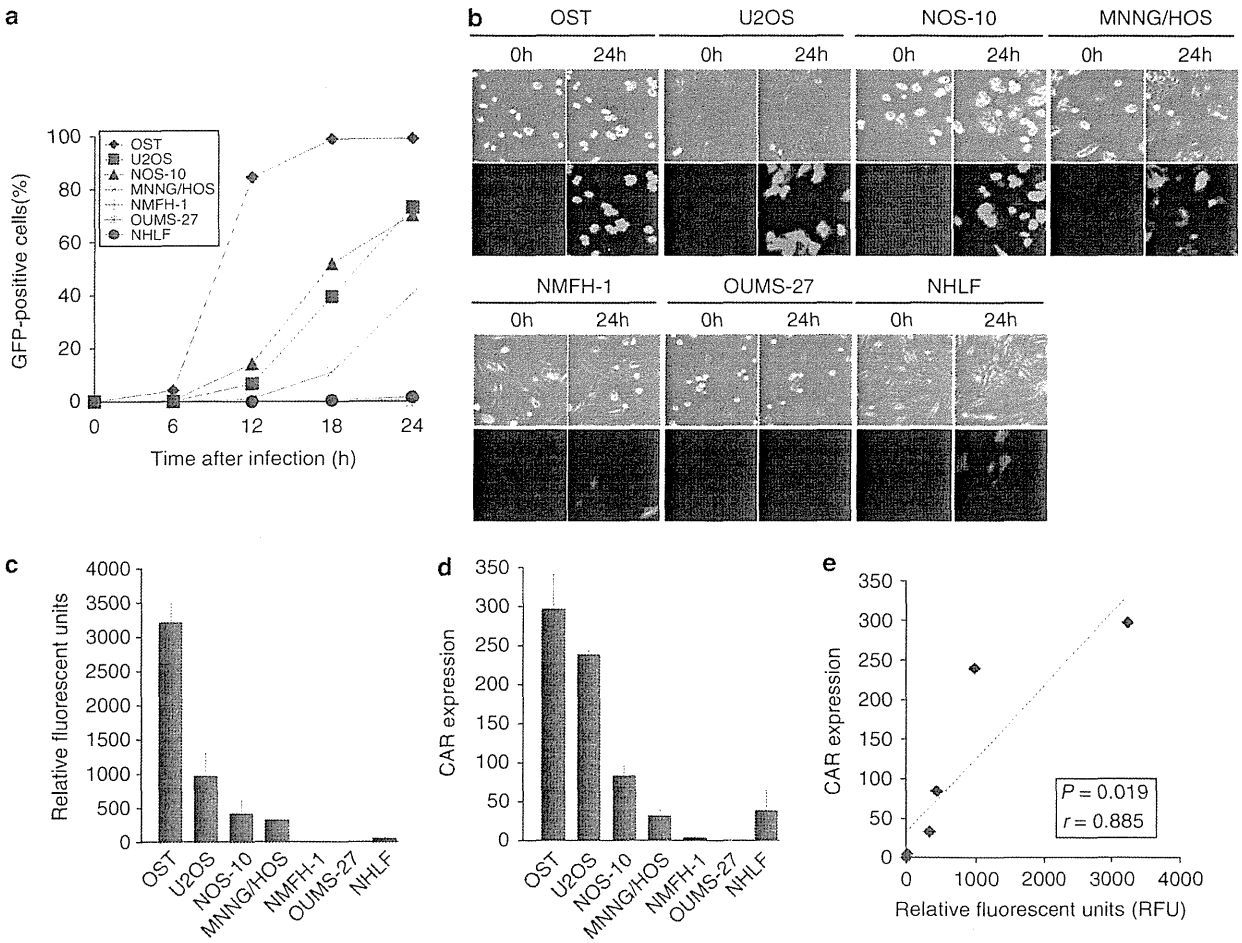

Figure 2. *In vitro* CAR-dependent GFP expression induced by OBP-401 infection. (**a**) The percentage of GFP-positive cells in all tumor and normal cells was counted at the indicated time points after OBP-301 infection at an MOI of 10 PFU per cell. (**b**) Time-lapse images of all tumor and normal cells were recorded for 24 h after infection with OBP-401 at an MOI of 10 PFU per cell. Representative images taken at the indicated time points show cell morphology that was analyzed using phase-contrast microscopy (top panels) and GFP expression that was analyzed using fluorescence microscopy (bottom panels). Original magnification: ×80. (**c**) Quantitative assessment of the level of GFP fluorescence in all tumor and normal cells 24 after OBP-401 infection at an MOI of 10 PFU per cell, using a fluorescent microplate reader with excitation/emission at 485 nm/528 nm. The intensity of GFP fluorescence was evaluated based on the brightness determinations used as relative fluorescence units (RFU). (**d**) The mean fluorescent intensity (MFI) of (CAR) expression on human sarcoma cells and normal fibroblasts. The cells were incubated with a monoclonal anti-CAR (RmcB) antibody, followed by a FITC-labeled secondary antibody, and were analyzed using flow cytometry. (**e**) Relationship between the level of GFP fluorescence and CAR expression in all tumor and normal cells after OBP-401 infection. The slope represents the inverse correlation between these two factors. Statistical significance was determined as $P<0.05$, after analysis of Pearson's correlation coefficient.

We previously reported that OBP-401 can efficiently induce GFP expression in small populations of metastatic tumor cells at various regions *in vivo*.[32-35] In this study, we further demonstrated that OBP-401-mediated GFP expression provides us the important information for detection of CAR-positive tumor cells. OBP-401 with *hTERT* gene promoter-induced GFP expression in CAR-positive tumor cells with telomerase activity, but not CAR-positive normal cells without telomerase activity (Figure 2c). There was significant relationship between the CAR expression and the GFP expression in tumor cells (Figure 2d). Among the four CAR-positive tumor cells, U2OS cells showed low GFP expression compared with high CAR expression (Figure 1a and 2c). As we recently reported that U2OS cells showed low *hTERT* mRNA expression, the low activity of *hTERT* gene promoter in tumor cells would affect OBP-401-mediated GFP expression. However, as various types of human cancer cells frequently show high telomerase activities,[39] OBP-401-mediated GFP induction system would be widely useful method to evaluate CAR expression in tumor cells.

Previous reports have suggested that *ex vivo* infection of human cancer specimens with a GFP-expressing replication-deficient adenovirus[40] or a replication-selective oncolytic adenovirus[41] is a useful method for assessment of the transduction efficacy or cytopathic activity, respectively, of Ad5-based vectors in individual tumor tissues. In this study, we confirmed that the GFP-expressing telomerase-specific oncolytic adenovirus OBP-401 is useful for detection of CAR-positive tumor tissues through induction of GFP expression (Figure 3b). Interestingly, OBP-401-infected OST tumor tissues showed heterogenous GFP expression (Figure 3b), although GFP expression was induced in all OBP-401-infected OST cells *in vitro* (Figure 2b). Our finding of heterogenous GFP expression in tumor tissues, which indicates heterogenous CAR expression, is consistent with a previously reported heterogeneity in CAR expression.[42] As several factors such as hypoxia[43] and cell cycle status[44] have been suggested to affect CAR expression in tumor cells, factors in the tumor microenvironment may be involved in the heterogenous CAR expression in tumor cells.

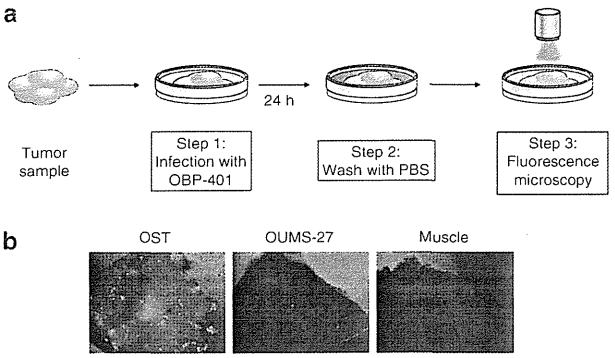

Figure 3. A simple method for detection of CAR expression in tumor tissues using OBP-401 infection. (**a**) Outline of the 3-step procedure; step 1: infection with OBP-401, step 2: washing with PBS and step 3: observation under a fluorescence microscope. Tumor tissues ($2 \times 2 \times 2\,mm^3$) were infected with OBP-401 at a concentration of 2.4×10^6 PFU for 24 h, were washed with PBS and were observed using fluorescence microscopy. (**b**) Assessment of GFP expression in the CAR-positive OST tumor (left panel), the CAR-negative OUMS-27 tumor (middle panel) and normal muscle tissues (right panel) under a fluorescence microscope. Original magnification: × 30.

Furthermore, as OBP-401 induces tumor-specific GFP expression, normal stromal or epithelial cells may be involved in heterogenous GFP expression in tumor tissues.

In conclusion, we have demonstrated that the GFP-expressing telomerase-specific replication-competent adenovirus OBP-401 is a promising fluorescence imaging tool for the detection of functional and tumor-specific CAR expression in tumor tissues. OBP-401-mediated GFP induction is a simple and highly sensitive method for analysis of tumor cells compared with conventional methods. This novel CAR detection system using OBP-401 has the potential of being widely applicable to assessment of predictive biomarkers for Ad5-based vector-mediated anticancer therapy.

MATERIALS AND METHODS

Cell lines

The human osteosarcoma cell line OST was kindly provided by Dr Satoru Kyo (Kanazawa University, Ishikawa, Japan). The human osteosarcoma cell line U2OS and the transformed embryonic kidney cell line 293 were obtained from the American Type Culture Collection (ATCC; Manassas, VA, USA). The human osteosarcoma cell line NOS-10[45] and the human malignant fibrous histiocytoma cell line NMFH-1[46] were kindly provided by Dr Hiroyuki Kawashima (Niigata University, Niigata, Japan). The human osteosarcoma cell line MNNG/HOS was purchased from DS Pharma Biomedical (Osaka, Japan). The chondrosarcoma cell line OUMS-27 was previously established in our laboratory.[47] The normal human lung fibroblast cell line NHLF was obtained from TaKaRa Biomedicals (Kyoto, Japan). These cells were propagated as monolayer cultures in the medium recommended by the manufacturer. All media were supplemented with 10% heat-inactivated fetal bovine serum, 100 units ml^{-1} penicillin and 100 μg ml^{-1} streptomycin. The cells were maintained at 37 °C in a humidified atmosphere containing 5% CO_2.

Recombinant adenoviruses

We previously generated and characterized OBP-401, which is a telomerase-specific replication-competent adenovirus variant, in which the *hTERT* promoter element drives the expression of *E1A* and *E1B* genes that are linked to an internal ribosome entry site, and in which the *GFP* gene is inserted into the E3 region under a cytomegalovirus promoter.[32,34] The virus was purified by ultracentrifugation using cesium chloride step gradients. Viral titers were determined by a plaque-forming assay using 293 cells and viruses were stored at −80 °C.

Flow cytometry

The cells (5×10^5 cells) were labeled with the mouse monoclonal anti-CAR (RmcB; Upstate Biotechnology, Lake Placid, NY, USA) antibody for 30 min at 4 °C. The cells were then incubated with fluorescent isothiocyanate-conjugated rabbit anti-mouse IgG second antibody (Zymed Laboratories, San Francisco, CA, USA) and were analyzed using flow cytometry (FACS Array; Becton Dickinson, Mountain View, CA, USA). The mean fluorescence intensity of CAR for each cell line was determined by calculating the differences between the mean fluorescence intensity in antibody-treated and non-treated cells in triplicate experiments.

Time-lapse confocal laser microscopy

The cells (1×10^5 cells per dish) were seeded in 35 mm glass-based dishes 20 h before virus infection. OST cells were infected with OBP-401 at an MOI of 1, 10 or 100 PFU per cell for 24 h. NMFH-1 and OUMS-27 cells were infected with OBP-401 at an MOI of 10 or 100 PFU per cell for 60 h. Other cells were infected with OBP-401 at an MOI of 10 PFU per cell for 24 h. Phase-contrast and fluorescence time-lapse recordings were obtained to concomitantly analyze cell morphology and GFP expression using an inverted FV10i confocal laser scanning microscopy (OLYMPUS; Tokyo, Japan). Photographic images were taken every 5 min. The percentage of GFP-positive cells in each field was calculated using the formula: the number of CAR-positive cells / the total number of CAR-positive and CAR-negative cells × 100.

Fluorescence microplate assay

The cells (5×10^3 cells per well) were seeded on 96-well black bottomed culture plates and were incubated for 20 h before virus infection. The cells were infected with OBP-401 at an MOI of 10 for 24 h. The level of expression of GFP fluorescence was measured using a fluorescent microplate reader (DS Pharma Biomedical; Osaka, Japan) with excitation/emission at 485 nm/528 nm. The mean expression of GFP fluorescence in each cell was calculated in triplicate experiments, as previously reported.[34]

Animal experiments

Animal experimental protocols were approved by the Ethics Review Committee for Animal Experimentation of Okayama University School of Medicine. OST and OUMS-27 cells (5×10^6 cells per site) were inoculated into the flank of female athymic nude mice aged 6 to 7 weeks (Charles River Laboratories, Wilmington, MA, USA). Palpable tumors developed within 14 to 21 days and were permitted to grow to ~5 to 6 mm in diameter. At that stage, tumor and normal muscle tissues were resected. The tumor and normal tissues ($2 \times 2 \times 2\,mm^3$) were placed in 96-well plates with culture medium. As single tumor cell is about 10 μm in diameter, we considered that there are 2.4×10^5 cells on the surface area of each sample tissue. Then, we infected each sample tissue with 2.4×10^6 PFU (10 MOI per sample) of OBP-401 for 24 h. After washing with PBS, tumor and normal tissues were again placed in 96-well plates with culture medium and analyzed using an inverted fluorescence microscope (OLYMPUS).

Statistical analysis

Data are expressed as means ± s.d. Student's *t*-test was used to compare differences between groups. Pearson's product-moment correlation coefficients were calculated using PASW statistics software version 18 (SPSS Inc., Chicago, IL, USA). Statistical significance was defined as when the *P* value was less than 0.05.

ABBREVIATIONS

Ad5, Adenovirus serotype 5; CAR, coxsackie and adenovirus receptor; GFP, green fluorescent protein; RT-PCR, reverse transcription-polymerase chain reaction; hTERT, human telomerase reverse transcriptase; MOI, multiplicity of infection;

PFU, plaque-forming unit; IRES, internal ribosome entry site; FITC, fluorescent isothiocyanate; MFI, mean fluorescence intensity.

CONFLICT OF INTEREST

Y Urata is an employee of Oncolys BioPharma, Inc., the manufacturer of OBP-401 (Telomescan). The remaining authors declare no conflict of interest.

ACKNOWLEDGEMENTS

We thank Dr Satoru Kyo (Kanazawa University) for providing the OST cells; Dr Hiroyuki Kawashima (Niigata University) for providing the NOS-10 and NMFH-1 cells; and Tomoko Sueishi for her excellent technical support. This study was supported by grants-in-Aid from the Ministry of Education, Science and Culture, Japan and grants from the Ministry of Health and Welfare, Japan.

REFERENCES

1 Kanerva A, Hemminki A. Adenoviruses for treatment of cancer. *Ann Med* 2005; **37**: 33-43.
2 Rein DT, Breidenbach M, Curiel DT. Current developments in adenovirus-based cancer gene therapy. *Future Oncol* 2006; **2**: 137-143.
3 Yamamoto M, Curiel DT. Current issues and future directions of oncolytic adenoviruses. *Mol Ther* 2010; **18**: 243-250.
4 Clayman GL, el-Naggar AK, Lippman SM, Henderson YC, Frederick M, Merritt JA *et al.* Adenovirus-mediated p53 gene transfer in patients with advanced recurrent head and neck squamous cell carcinoma. *J Clin Oncol* 1998; **16**: 2221-2232.
5 Swisher SG, Roth JA, Nemunaitis J, Lawrence DD, Kemp BL, Carrasco CH *et al.* Adenovirus-mediated p53 gene transfer in advanced non-small-cell lung cancer. *J Natl Cancer Inst* 1999; **91**: 763-771.
6 Shimada H, Matsubara H, Shiratori T, Shimizu T, Miyazaki S, Okazumi S *et al.* Phase I/II adenoviral p53 gene therapy for chemoradiation resistant advanced esophageal squamous cell carcinoma. *Cancer Sci* 2006; **97**: 554-561.
7 Fujiwara T, Tanaka N, Kanazawa S, Ohtani S, Saijo Y, Nukiwa T *et al.* Multicenter phase I study of repeated intratumoral delivery of adenoviral p53 in patients with advanced non-small-cell lung cancer. *J Clin Oncol* 2006; **24**: 1689-1699.
8 Fujiwara T, Urata Y, Tanaka N. Telomerase-specific oncolytic virotherapy for human cancer with the hTERT promoter. *Curr Cancer Drug Targets* 2007; **7**: 191-201.
9 Pesonen S, Kangasniemi L, Hemminki A. Oncolytic adenoviruses for the treatment of human cancer: focus on translational and clinical data. *Mol Pharm* 2011; **8**: 12-28.
10 Bergelson JM, Cunningham JA, Droguett G, Kurt-Jones EA, Krithivas A, Hong JS *et al.* Isolation of a common receptor for Coxsackie B viruses and adenoviruses 2 and 5. *Science* 1997; **275**: 1320-1323.
11 Hemmi S, Geertsen R, Mezzacasa A, Peter I, Dummer R. The presence of human coxsackievirus and adenovirus receptor is associated with efficient adenovirus-mediated transgene expression in human melanoma cell cultures. *Hum Gene Ther* 1998; **9**: 2363-2373.
12 Hutchin ME, Pickles RJ, Yarbrough WG. Efficiency of adenovirus-mediated gene transfer to oropharyngeal epithelial cells correlates with cellular differentiation and human coxsackie and adenovirus receptor expression. *Hum Gene Ther* 2000; **11**: 2365-2375.
13 You Z, Fischer DC, Tong X, Hasenburg A, Aguilar-Cordova E, Kieback DG. Coxsackievirus-adenovirus receptor expression in ovarian cancer cell lines is associated with increased adenovirus transduction efficiency and transgene expression. *Cancer Gene Ther* 2001; **8**: 168-175.
14 Rauen KA, Sudilovsky D, Le JL, Chew KL, Hann B, Weinberg V *et al.* Expression of the coxsackie adenovirus receptor in normal prostate and in primary and metastatic prostate carcinoma: potential relevance to gene therapy. *Cancer Res* 2002; **62**: 3812-3818.
15 Kim M, Zinn KR, Barnett BG, Sumerel LA, Krasnykh V, Curiel DT *et al.* The therapeutic efficacy of adenoviral vectors for cancer gene therapy is limited by a low level of primary adenovirus receptors on tumour cells. *Eur J Cancer* 2002; **38**: 1917-1926.
16 Qin M, Chen S, Yu T, Escuadro B, Sharma S, Batra RK. Coxsackievirus adenovirus receptor expression predicts the efficiency of adenoviral gene transfer into non-small cell lung cancer xenografts. *Clin Cancer Res* 2003; **9**: 4992-4999.
17 Douglas JT, Kim M, Sumerel LA, Carey DE, Curiel DT. Efficient oncolysis by a replicating adenovirus (ad) *in vivo* is critically dependent on tumor expression of primary ad receptors. *Cancer Res* 2001; **61**: 813-817.
18 Fuxe J, Liu L, Malin S, Philipson L, Collins VP, Pettersson RF. Expression of the coxsackie and adenovirus receptor in human astrocytic tumors and xenografts. *Int J Cancer* 2003; **103**: 723-729.
19 Marsee DK, Vadysirisack DD, Morrison CD, Prasad ML, Eng C, Duh QY *et al.* Variable expression of coxsackie-adenovirus receptor in thyroid tumors: implications for adenoviral gene therapy. *Thyroid* 2005; **15**: 977-987.
20 Anders M, Rosch T, Kuster K, Becker I, Hofler H, Stein HJ *et al.* Expression and function of the coxsackie and adenovirus receptor in Barrett's esophagus and associated neoplasia. *Cancer Gene Ther* 2009; **16**: 508-515.
21 Korn WM, Macal M, Christian C, Lacher MD, McMillan A, Rauen KA *et al.* Expression of the coxsackievirus- and adenovirus receptor in gastrointestinal cancer correlates with tumor differentiation. *Cancer Gene Ther* 2006; **13**: 792-797.
22 Gu W, Ogose A, Kawashima H, Ito M, Ito T, Matsuba A *et al.* High-level expression of the coxsackievirus and adenovirus receptor messenger RNA in osteosarcoma, Ewing's sarcoma, and benign neurogenic tumors among musculoskeletal tumors. *Clin Cancer Res* 2004; **10**: 3831-3838.
23 Kawashima H, Ogose A, Yoshizawa T, Kuwano R, Hotta Y, Hotta T *et al.* Expression of the coxsackievirus and adenovirus receptor in musculoskeletal tumors and mesenchymal tissues: efficacy of adenoviral gene therapy for osteosarcoma. *Cancer Sci* 2003; **94**: 70-75.
24 Rice AM, Currier MA, Adams LC, Bharatan NS, Collins MH, Snyder JD *et al.* Ewing sarcoma family of tumors express adenovirus receptors and are susceptible to adenovirus-mediated oncolysis. *J Pediatr Hematol Oncol* 2002; **24**: 527-533.
25 Matsumoto K, Shariat SF, Ayala GE, Rauen KA, Lerner SP. Loss of coxsackie and adenovirus receptor expression is associated with features of aggressive bladder cancer. *Urology* 2005; **66**: 441-446.
26 Anders M, Vieth M, Rocken C, Ebert M, Pross M, Gretschel S *et al.* Loss of the coxsackie and adenovirus receptor contributes to gastric cancer progression. *Br J Cancer* 2009; **100**: 352-359.
27 Yamamoto S, Yoshida Y, Aoyagi M, Ohno K, Hirakawa K, Hamada H. Reduced transduction efficiency of adenoviral vectors expressing human p53 gene by repeated transduction into glioma cells *in vitro*. *Clin Cancer Res* 2002; **8**: 913-921.
28 Tango Y, Taki M, Shirakiya Y, Ohtani S, Tokunaga N, Tsunemitsu Y *et al.* Late resistance to adenoviral p53-mediated apoptosis caused by decreased expression of Coxsackie-adenovirus receptors in human lung cancer cells. *Cancer Sci* 2004; **95**: 459-463.
29 Sasaki T, Tazawa H, Hasei J, Kunisada T, Yoshida A, Hashimoto Y *et al.* Preclinical evaluation of telomerase-specific oncolytic virotherapy for human bone and soft tissue sarcomas. *Clin Cancer Res* 2011; **17**: 1828-1838.
30 Kawashima T, Kagawa S, Kobayashi N, Shirakiya Y, Umeoka T, Teraishi F *et al.* Telomerase-specific replication-selective virotherapy for human cancer. *Clin Cancer Res* 2004; **10** (1 Pt 1): 285-292.
31 Hashimoto Y, Watanabe Y, Shirakiya Y, Uno F, Kagawa S, Kawamura H *et al.* Establishment of biological and pharmacokinetic assays of telomerase-specific replication-selective adenovirus. *Cancer Sci* 2008; **99**: 385-390.
32 Kishimoto H, Kojima T, Watanabe Y, Kagawa S, Fujiwara T, Uno F *et al. In vivo* imaging of lymph node metastasis with telomerase-specific replication-selective adenovirus. *Nat Med* 2006; **12**: 1213-1219.
33 Kishimoto H, Urata Y, Tanaka N, Fujiwara T, Hoffman RM. Selective metastatic tumor labeling with green fluorescent protein and killing by systemic administration of telomerase-dependent adenoviruses. *Mol Cancer Ther* 2009; **8**: 3001-3008.
34 Kojima T, Hashimoto Y, Watanabe Y, Kagawa S, Uno F, Kuroda S *et al.* A simple biological imaging system for detecting viable human circulating tumor cells. *J Clin Invest* 2009; **119**: 3172-3181.
35 Kishimoto H, Zhao M, Hayashi K, Urata Y, Tanaka N, Fujiwara T *et al. In vivo* internal tumor illumination by telomerase-dependent adenoviral GFP for precise surgical navigation. *Proc Natl Acad Sci USA* 2009; **106**: 14514-14517.
36 Feero WG, Rosenblatt JD, Huard J, Watkins SC, Epperly M, Clemens PR *et al.* Viral gene delivery to skeletal muscle: insights on maturation-dependent loss of fiber infectivity for adenovirus and herpes simplex type 1 viral vectors. *Hum Gene Ther* 1997; **8**: 371-380.
37 Hoffman RM. The multiple uses of fluorescent proteins to visualize cancer *in vivo*. *Nat Rev Cancer* 2005; **5**: 796-806.
38 Hoffman RM, Yang M. Subcellular imaging in the live mouse. *Nat Protoc* 2006; **1**: 775-782.
39 Shay JW, Bacchetti S. A survey of telomerase activity in human cancer. *Eur J Cancer* 1997; **33**: 787-791.
40 Marsman WA, Buskens CJ, Wesseling JG, Offerhaus GJ, Bergman JJ, Tytgat GN *et al.* Gene therapy for esophageal carcinoma: the use of an explant model to test adenoviral vectors *ex vivo*. *Cancer Gene Ther* 2004; **11**: 289-296.
41 Wang Y, Thorne S, Hannock J, Francis J, Au T, Reid T *et al.* A novel assay to assess primary human cancer infectibility by replication-selective oncolytic adenoviruses. *Clin Cancer Res* 2005; **11**: 351-360.
42 Zeimet AG, Muller-Holzner E, Schuler A, Hartung G, Berger J, Hermann M *et al.* Determination of molecules regulating gene delivery using adenoviral vectors in ovarian carcinomas. *Gene Therapy* 2002; **9**: 1093-1100.
43 Kuster K, Koschel A, Rohwer N, Fischer A, Wiedenmann B, Anders M. Downregulation of the coxsackie and adenovirus receptor in cancer cells by hypoxia depends on HIF-1alpha. *Cancer Gene Ther* 2010; **17**: 141-146.

44 Seidman MA, Hogan SM, Wendland RL, Worgall S, Crystal RG, Leopold PL. Variation in adenovirus receptor expression and adenovirus vector-mediated transgene expression at defined stages of the cell cycle. *Mol Ther* 2001; **4**: 13-21.

45 Hotta T, Motoyama T, Watanabe H. Three human osteosarcoma cell lines exhibiting different phenotypic expressions. *Acta Pathol Jpn* 1992; **42**: 595-603.

46 Kawashima H, Ogose A, Gu W, Nishio J, Kudo N, Kondo N *et al.* Establishment and characterization of a novel myxofibrosarcoma cell line. *Cancer Genet Cytogenet* 2005; **161**: 28-35.

47 Kunisada T, Miyazaki M, Mihara K, Gao C, Kawai A, Inoue H *et al.* A new human chondrosarcoma cell line (OUMS-27) that maintains chondrocytic differentiation. *Int J Cancer* 1998; **77**: 854-859.

Supplementary Information accompanies the paper on Gene Therapy website (http://www.nature.com/gt)

Molecular Cancer Therapeutics

Dual Programmed Cell Death Pathways Induced by p53 Transactivation Overcome Resistance to Oncolytic Adenovirus in Human Osteosarcoma Cells

Joe Hasei[1], Tsuyoshi Sasaki[1], Hiroshi Tazawa[2,4], Shuhei Osaki[1], Yasuaki Yamakawa[1], Toshiyuki Kunisada[1,3], Aki Yoshida[1], Yuuri Hashimoto[2], Teppei Onishi[2], Futoshi Uno[2], Shunsuke Kagawa[2], Yasuo Urata[5], Toshifumi Ozaki[1], and Toshiyoshi Fujiwara[2]

Abstract

Tumor suppressor p53 is a multifunctional transcription factor that regulates diverse cell fates, including apoptosis and autophagy in tumor biology. p53 overexpression enhances the antitumor activity of oncolytic adenoviruses; however, the molecular mechanism of this occurrence remains unclear. We previously developed a tumor-specific replication-competent oncolytic adenovirus, OBP-301, that kills human osteosarcoma cells, but some human osteosarcoma cells were OBP-301–resistant. In this study, we investigated the antitumor activity of a p53-expressing oncolytic adenovirus, OBP-702, and the molecular mechanism of the p53-mediated cell death pathway in OBP-301–resistant human osteosarcoma cells. The cytopathic activity of OBP-702 was examined in OBP-301–sensitive (U2OS and HOS) and OBP-301–resistant (SaOS-2 and MNNG/HOS) human osteosarcoma cells. The molecular mechanism in the OBP-702–mediated induction of two cell death pathways, apoptosis and autophagy, was investigated in OBP-301–resistant osteosarcoma cells. The antitumor effect of OBP-702 was further assessed using an orthotopic OBP-301–resistant MNNG/HOS osteosarcoma xenograft tumor model. OBP-702 suppressed the viability of OBP-301–sensitive and -resistant osteosarcoma cells more efficiently than OBP-301 or a replication-deficient p53-expressing adenovirus (Ad-p53). OBP-702 induced more profound apoptosis and autophagy when compared with OBP-301 or Ad-p53. E1A-mediated *miR-93/106b* upregulation induced p21 suppression, leading to p53-mediated apoptosis and autophagy in OBP-702–infected cells. p53 overexpression enhanced adenovirus-mediated autophagy through activation of damage-regulated autophagy modulator (DRAM). Moreover, OBP-702 suppressed tumor growth in an orthotopic OBP-301–resistant MNNG/HOS xenograft tumor model. These results suggest that OBP-702–mediated p53 transactivation is a promising antitumor strategy to induce dual apoptotic and autophagic cell death pathways via regulation of miRNA and DRAM in human osteosarcoma cells. *Mol Cancer Ther; 12(3); 314–25. ©2012 AACR.*

Introduction

Osteosarcoma is one of the most common malignant tumors in young children (1, 2). Current treatment strategies, which consist of multi-agent chemotherapy and aggressive surgery, have significantly improved the cure rate and prognosis of patients with osteosarcoma. In fact, over the past 30 years, the 5-year survival rate has increased from 10% to 70% (3–5). Even in patients with osteosarcoma with metastases at diagnosis, the 5-year survival rate has reached 20% to 30% in response to chemotherapy and surgical removal of primary and metastatic tumors (6). However, treatment outcomes for patients with osteosarcomas have further improved over the last few years. Therefore, the development of novel therapeutic strategies is required to improve the clinical outcomes in patients with osteosarcomas.

Tumor-specific replication-competent oncolytic viruses are being developed as novel anticancer therapy, in which the promoters of cancer-related genes are used to regulate virus replication in a tumor-dependent manner. More than 85% of all human cancers express high telomerase activity to maintain the length of the telomeres during cell division, whereas normal somatic cells seldom show this enhanced telomerase activity (7, 8). Telomerase activity has also been detected in 44% to 81% of bone and

Authors' Affiliations: Departments of [1]Orthopaedic Surgery, [2]Gastroenterological Surgery, and [3]Medical Materials for Musculoskeletal Reconstruction, Okayama University Graduate School of Medicine, Dentistry and Pharmaceutical Sciences; [4]Center for Innovative Clinical Medicine, Okayama University Hospital, Okayama; and [5]Oncolys BioPharma, Inc., Tokyo, Japan

Note: Supplementary data for this article are available at Molecular Cancer Therapeutics Online (http://mct.aacrjournals.org/).

Corresponding Author: Toshiyoshi Fujiwara, Department of Gastroenterological Surgery, Okayama University Graduate School of Medicine, Dentistry and Pharmaceutical Sciences, 2-5-1 Shikata-cho, Kita-ku, Okayama 700-8558, Japan. Phone: 81-86-235-7257; Fax: 81-86-221-8775; E-mail: toshi_f@md.okayama-u.ac.jp

doi: 10.1158/1535-7163.MCT-12-0869

soft-tissue sarcomas (9, 10). Telomerase activation is closely correlated with the expression of the human telomerase reverse transcriptase (*hTERT*) gene (11). On the basis of these data, we previously developed a telomerase-specific replication-competent oncolytic adenovirus OBP-301 (Telomelysin) in which the *hTERT* gene promoter drives the expression of the *E1A* and *E1B* genes (12). A phase I clinical trial of OBP-301, which was conducted in the United States on patients with advanced solid tumors, indicated that OBP-301 was well tolerated by patients (13). Recently, we reported that OBP-301 efficiently killed human bone and soft-tissue sarcoma cells (14, 15). However, some osteosarcoma cell lines were not sensitive to the antitumor effect of OBP-301. Therefore, to efficiently eliminate tumor cells with OBP-301, its antitumor effects need to be enhanced.

Cancer gene therapy is defined as the treatment of malignant tumors via the introduction of a therapeutic tumor suppressor gene or the abrogation of an oncogene. The tumor suppressor *p53* gene has an attractive tumor suppressor profile as a potent therapeutic transgene for induction of cell-cycle arrest, senescence, apoptosis, and autophagy (16). Dual cell death pathways, such as apoptosis and autophagy, induced by p53 transactivation are mainly involved in the suppression of tumor initiation and progression. However, among the p53 downstream target genes, p21, which is most rapidly and strongly induced during the DNA damage response, mainly induces cell-cycle arrest through suppression of apoptotic and autophagic cell death pathways (17, 18). Thus, p21 suppression may be a more effective strategy for the induction of apoptotic and autophagic cell death pathways in tumor cells, particularly when the tumor suppressor *p53* gene is overexpressed in tumor cells in response to cancer gene therapy.

A p53-expressing replication-deficient adenovirus (Ad-p53, Advexin) has previously been reported to induce an antitumor effect in the *in vitro* and *in vivo* settings (19, 20) as well as in some clinical studies (21–24). We recently reported that combination therapy with OBP-301 and Ad-p53 resulted in a more profound antitumor effect than monotherapy with either OBP-301 or Ad-p53 (25). Moreover, we generated armed OBP-301 expressing the wild-type *p53* tumor suppressor gene (OBP-702) and showed that OBP-702 suppressed the viability of various types of epithelial malignant cells more efficiently than did OBP-301 (26). OBP-702 induced a more profound apoptotic cell death effect than Ad-p53, likely via adenoviral E1A-mediated suppression of anti-apoptotic p21 in human epithelial malignant cells. However, it remained unclear whether OBP-702 efficiently induces an antitumor effect in human nonepithelial malignant cells, including osteosarcomas.

In the present study, we investigated the *in vitro* cytopathic efficacy of the p53-expressing telomerase-specific replication-competent oncolytic adenovirus, OBP-702, in human osteosarcoma cells, and we compared the induction level of apoptotic and autophagic cell deaths in OBP-301–resistant human osteosarcoma cells infected with OBP-301, OBP-702, and Ad-p53. The molecular mechanism by which OBP-702 mediates induction of apoptosis and autophagy was also investigated. Finally, the *in vivo* antitumor effect of OBP-702 was evaluated using an orthotopic OBP-301–resistant human osteosarcoma xenograft tumor model.

Materials and Methods

Cell lines

The human osteosarcoma cell lines, HOS and SaOS-2, were kindly provided by Dr. Satoru Kyo (Kanazawa University, Ishikawa, Japan). These cells were propagated as monolayer cultures in Dulbecco's Modified Eagle's Medium. The human osteosarcoma cell line, U2OS, was obtained from the American Type Culture Collection and was grown in McCoy's 5a Medium. The human osteosarcoma cell line, MNNG/HOS, was purchased from DS Pharma Biomedical and was maintained in Eagle's Minimum Essential Medium containing 1% nonessential amino acids. All media were supplemented with 10% FBS, 100 U/mL penicillin, and 100 mg/mL streptomycin. The normal human lung fibroblast (NHLF) cell line, NHLF, was obtained from TaKaRa Biomedicals. NHLF cells were propagated as monolayer culture in the medium recommended by the manufacturer. Although cell lines were not authenticated by the authors, cells were immediately expanded after receipt and stored in liquid N_2. Cells were not cultured for more than 5 months following resuscitation. The cells were maintained at 37°C in a humidified atmosphere with 5% CO_2.

Recombinant adenoviruses

The recombinant telomerase-specific replication-competent adenovirus OBP-301 (Telomelysin), in which the promoter element of the *hTERT* gene drives the expression of *E1A* and *E1B* genes, was previously constructed and characterized (12, 27). For OBP-301–mediated induction of exogenous *p53* gene expression, we recently generated OBP-702, in which a human wild-type *p53* gene expression cassette was inserted into the *E3* region (Supplementary Fig. S1; ref. 26). Ad-p53 is a replication-defective adenovirus serotype 5 vector with a *p53* gene expression cassette at the *E1* region (19, 20). Recombinant viruses were purified by ultracentrifugation using cesium chloride step gradients, their titers were determined by a plaque-forming assay using 293 cells and they were stored at −80°C.

Cell viability assay

Cells were seeded on 96-well plates at a density of 1×10^3 cells/well 24 hours before viral infection. All cell lines were infected with OBP-702 at multiplicity of infections (MOI) of 0, 0.1, 1, 10, 50, or 100 plaque-forming units (PFU)/cell. Cell viability was determined on days 1, 2, 3, and 5 after virus infection using Cell Proliferation Kit II (Roche Molecular Biochemicals). The 50% inhibiting dose (ID_{50}) value of OBP-702 for each cell line was calculated

using cell viability data obtained on day 5 after virus infection.

Time-lapse confocal laser microscopy

GFP-expressing MNNG/HOS (MNNG/HOS-GFP) cells were established by stable transfection with GFP expression plasmid using Lipofectamine LTX (Invitrogen). MNNG/HOS-GFP and NHLF cells were seeded in 35-mm glass-based dishes at a density of 1×10^5 cells/dish 24 hours before infection and were infected with OBP-702 at an MOI of 10 PFU/cell for 72 hours. Phase-contrast and fluorescence time-lapse recordings were obtained to concomitantly analyze cell morphology and GFP expression using an inverted FV10i confocal laser scanning microscopy (OLYMPUS).

Western blot analysis

SaOS-2 and MNNG/HOS cells, seeded in a 100-mm dish at a density of 1×10^5 cells/dish, were infected with OBP-301, OBP-702, or Ad-p53 at the indicated MOIs. In contrast, SaOS-2 cells were transfected with 10 nmol/L *miR-93* (Ambion), *miR-106b* (Ambion), or control miRNA (Ambion) 24 hours before Ad-p53 infection and infected with Ad-p53 at an MOI of 100 for 48 hours. Whole-cell lysates were prepared in a lysis buffer [50 mmol/L Tris-HCl (pH 7.4), 150 mmol/L NaCl, 1% Triton X-100] containing a protease inhibitor cocktail (Complete Mini; Roche) at the indicated time points. Proteins were electrophoresed on 6% to 15% SDS-PAGE and were transferred to polyvinylidene difluoride membranes (Hybond-P; GE Health Care). Blots were blocked with 5% non-fat dry milk in TBS-T (Tris-buffered saline and 0.1% Tween-20, pH 7.4). The primary antibodies used were: rabbit anti-PARP polyclonal antibody (pAb; Cell Signaling Technology), mouse anti-p53 monoclonal antibody (mAb; Calbiochem), mouse anti-$p21^{WAF1}$ mAb (Calbiochem), rabbit anti-E2F1 pAb (Santa Cruz Biotechnology), mouse anti-Ad5 E1A mAb (BD PharMingen), rabbit anti-microtubule-associated protein 1 light chain 3 (LC3) pAb [Medical & Biological Laboratories (MBL)], mouse anti-p62 mAb (MBL), rabbit anti-damage-regulated autophagy modulator (DRAM) pAb (Abgent), and mouse anti-β-actin mAb (Sigma-Aldrich).

Flow cytometric analysis

To analyze the active caspase-3 expression, cells were incubated for 20 minutes on ice in Cytofix/Cytoperm solution (BD Biosciences), labeled with phycoerythrin (PE)-conjugated rabbit anti-active caspase-3 mAb (BD Biosciences) for 30 minutes, and then analyzed using FACS array (BD Biosciences).

To evaluate the sub-G_1 population, which is a apoptosis indicator, in SaOS-2 cells after virus infection, SaOS-2 cells were seeded in a 100-mm dish at a density of 1×10^6 cells/dish 24 hours before viral infection and were infected with mock, OBP-301, Ad-p53, or OBP-702 at an MOI of 10 PFUs/cell for 48 hours. Cells were trypsinized and resuspended in original supernatant to ensure that both attached and nonattached cells were analyzed. Cells stained with propidium iodide were analyzed using FACS array (BD Biosciences).

Quantitative real-time reverse transcription PCR analysis

To evaluate the expressions of *miR-93* and *miR-106b* in tumor cells after OBP-702 infection, SaOS-2 and MNNG/HOS cells were seeded on 6-well plates at a density of 2×10^5 cells/well 24 hours before viral infection and were infected with OBP-702 at MOIs of 0, 1, 5, 10, 50, or 100 PFU/cell. Three days after virus infection, total RNA was extracted from the cells using a miRNeasy Mini Kit (Qiagen). The concentration and quality of RNA were assessed using a Nanodrop spectrophotometer. cDNA was synthesized from 10 ng of total RNA using the TaqMan MicroRNA Reverse Transcription Kit (Applied Biosystems), and quantitative real-time reverse transcription (RT)-PCR was carried out using the Applied Biosystems StepOnePlus real-time PCR System. The expressions of *miR-93* and *miR-106b* were defined from the threshold cycle (C_t), and relative expression levels were calculated using the $2^{-\Delta\Delta C_t}$ method after normalization with reference to the expression of U6 small nuclear RNA.

***In vivo* orthotopic MNNG/HOS xenograft tumor model**

Animal experimental protocols were approved by the Ethics Review Committee for Animal Experimentation of Okayama University School of Medicine (Okayama, Japan). MNNG/HOS cells (5×10^6 cells per site) were inoculated into the tibias of female athymic nude mice aged 6 to 7 weeks (CLEA Japan). Palpable tumors developed within 21 days and were permitted to grow to approximately 5 to 6 mm in diameter. At that stage, a 50-μL volume of solution containing OBP-702, OBP-301, or Ad-p53 at a dose of 1×10^8 PFU or PBS was injected into the tumors for 3 cycles every 2 days. Tumor volume was monitored by computed tomographic (CT) imaging once a week after virus infection.

Three-dimensional computed tomography imaging

The tumor volume and formation of osteolytic lesions were evaluated using three-dimensional CT (3D-CT) imaging (ALOKA Latheta LCT-200; Hitachi Aloka Medical). The tumor volume was calculated by INTAGE Realia software (Cybernet Systems).

Histopathologic analysis

Tumors were fixed in 10% neutralized formalin and embedded in paraffin blocks. Sections were stained with hematoxylin/eosin and analyzed by light microscopy.

Statistical analysis

Data are expressed as means ± SD. Student *t* test was used to compare differences between groups. Statistical significance was defined as $P < 0.05$.

Results

In vitro cytopathic efficacy of OBP-702 against human osteosarcoma cell lines

To evaluate the *in vitro* cytopathic activity of OBP-702, we used the 2 OBP-301–sensitive human osteosarcoma cells (HOS and U2OS) and the 2 OBP-301–resistant human osteosarcoma cells (SaOS-2 and MNNG/HOS) that were recently described (14). The cell viability of each cell was assessed over 5 days after infection using the XTT assay. OBP-702 infection suppressed the viability of OBP-301–sensitive and -resistant cells in dose- and time-dependent manners (Fig. 1A and B). When the ID_{50} values of OBP-702 in all 4 human osteosarcoma cells were compared with those of OBP-301 calculated in a previous report (14), all cell lines were more sensitive to OBP-702 than to OBP-301 (Table 1). The ID_{50} values of OBP-702 were also lower than those of Ad-p53 (Supplementary Fig. S2). However, OBP-702 did not exhibit any cytopathic effect in NHLF cells (Fig. 1B). When GFP-expressing MNNG/HOS-GFP cells were cocultured with human normal NHLF cells, OBP-702 infection showed a cytopathic effect (confirmed by observation of round-shaped morphologic changes) in MNNG/HOS-GFP cells but not in NHLF cells (Fig. 1C). These results indicate that OBP-702 was more cytopathic than OBP-301 for human osteosarcoma cells but was not cytopathic for normal human cells.

Increased induction of apoptosis by OBP-702 when compared with OBP-301 or Ad-p53

We next investigated whether OBP-702 induces more profound apoptosis when compared with OBP-301 or Ad-p53. OBP-301–resistant SaOS-2 and MNNG/HOS cells

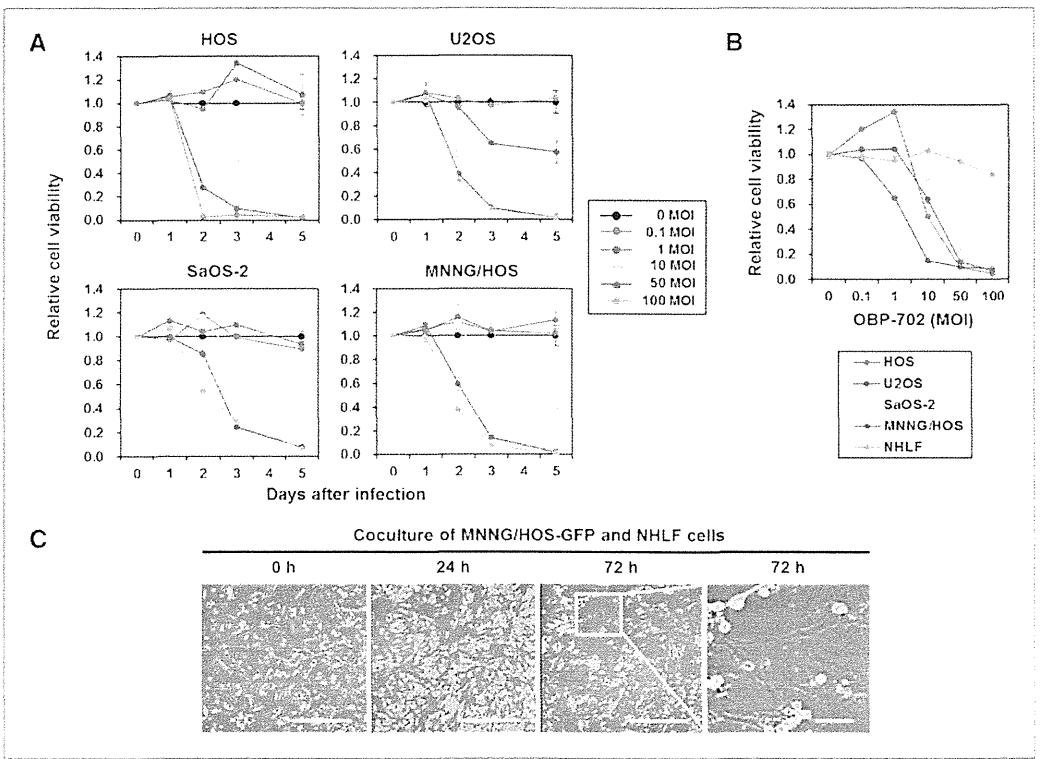

Figure 1. *In vitro* cytopathic effect of OBP-702 in human osteosarcoma cell lines. A, OBP-301–sensitive (HOS and U2OS) and OBP-301–resistant (SaOS-2 and MNNG/HOS) human osteosarcoma cells were infected with OBP-702 at the indicated MOI, and cell viability was quantified over 5 days using the XTT assay. Cell viability was calculated relative to that of the mock-infected group on each day, which was set at 1.0. Cell viability data are expressed as mean values ± SD ($n = 5$). B, four human osteosarcoma cells and one normal fibroblast NHLF cell were seeded 24 hours before viral infection and were infected with OBP-702 at the indicated MOIs, and cell viability was examined on day 5 using the XTT assay. Cell viability was calculated relative to that of the mock-infected group, which was set at 1.0. Cell viability data are expressed as mean ± SD ($n = 5$). C, time lapse images of cytopathic effect of OBP-702 in coculture of GFP-expressing MNNG/HOS cells with human normal fibroblast NHLF cells. MNNG/HOS-GFP cells coincubated with NHLF cells were recorded for 72 hours after OBP-702 infection at an MOI of 10. Three images on the left are low magnification and one image on the right is high magnification of the area outlined by a white square. Left scale bars, 100 μm. Right scale bar, 10 μm.

Table 1. Comparison of ID_{50} values of OBP-301 and OBP-702 in various human osteosarcoma cell lines

Cell lines	Sensitivity to OBP-301	Cell type	Relative hTERT mRNA expression	ID_{50} value[a] (MOI)		Ratio[b] (OBP-702/ OBP-301)
				OBP-301	OBP-702	
SaOS-2	Resistant	ALT	Negative	98.1	5.5	0.06
MNNG/HOS	Resistant	Non-ALT	1	97.3	6.7	0.07
U2OS	Sensitive	ALT	0.3	38.2	1.2	0.03
HOS	Sensitive	Non-ALT	4.3	43.0	4.5	0.10

[a]The ID_{50} values of OBP-702 and OBP-301 were calculated from the data of XTT assay on day 5 after infection.
[b]The ratio was calculated from the division of the ID_{50} value of OBP-702 by the ID_{50} value of OBP-301.

were infected with OBP-702, OBP-301, or Ad-p53, and apoptosis was assessed by Western blot and flow cytometric analyses. Western blot analysis showed that SaOS-2 cells exhibited the cleavage of PARP after infection with OBP-702 (>5 MOIs) or Ad-p53 (>50 MOIs), whereas MNNG/HOS cells had the cleavage of PARP after infection with OBP-702 (>5 MOIs) but not Ad-p53 (Fig. 2A). In contrast, OBP-301 did not induce apoptosis (data not shown). Furthermore, flow cytometric analysis showed that OBP-702 infection (10 MOIs) significantly increased the percentage of apoptotic cells with active caspase-3 when compared with Ad-p53 or OBP-301 at same doses in SaOS-2 and MNNG/HOS cells (Fig. 2B and C). Cell-cycle analysis also showed that OBP-702 (10 MOIs) induced the highest percentages of sub-G_1 population in SaOS-2 cells when compared with Ad-p53 or OBP-301 at same doses (Fig. 2D). These results suggest that OBP-702 induces increased apoptosis when compared with Ad-p53 or OBP-301 in human osteosarcoma cells.

p53 induction in human osteosarcoma cells infected with OBP-702

To investigate the molecular mechanism of OBP-702–induced apoptosis in human osteosarcoma cells, we evaluated p53 expression after OBP-702 infection in SaOS-2 (p53-null) and MNNG/HOS (p53-mutant) cells in which endogenous p53 expression level was confirmed by Western blot analysis (Supplementary Fig. S3). OBP-702 efficiently induced p53 expression in SaOS-2 and MNNG/HOS cells (Fig. 3A). The level of p53 expression was higher in OBP-702–treated cells than in Ad-p53–treated cells (Fig. 3A). Despite of OBP-702–induced high p53 expression, p53 downstream target p21 protein was induced only in Ad-p53–treated cells.

To investigate the effect of exogenous p53 overexpression in virus replication, we next compared the replication abilities of OBP-702 and OBP-301 in p53-null SaOS-2 cells by measuring the relative amounts of *E1A* copy numbers. The *E1A* copy number of OBP-702 was similar to that of OBP-301 in SaOS-2 cells (Supplementary Fig. S4). These results indicate that OBP-702 efficiently induces exogenous p53 expression without affecting p21 expression and virus replication in human osteosarcoma cells.

OBP-702–mediated upregulation of *miR-93* and *miR-106b* suppresses p21 expression

Adenoviral E1A protein has been shown to activate E2F1 expression (28), which is a multifunctional transcription factor that regulates diverse cell fates through induction of many target genes, including small noncoding miRNAs (29). Recently, E2F1-inducible *miR-93* and *miR-106b* have been shown to suppress p21 expression in human cancer cells (30). Therefore, we sought to investigate whether OBP-702 induces expressions of E2F1 and E2F1-regulated miRNAs (*miR-93* and *miR-106b*). OBP-702 infection activated E2F1 expression along with E1A accumulation in SaOS-2 and MNNG/HOS cells (Fig. 3B). The expression levels of *miR-93* and *miR-106b* were increased in association with E2F1 activation in OBP-702–infected SaOS-2 and MNNG/HOS cells (Fig. 3C). In contrast, E1A-deleted Ad-p53 infection did not increase expressions of E2F1 and E2F1-regulated *miR-93* and *miR-106b* (data not shown). Next, we assessed whether upregulation of *miR-93* and *miR-106b* efficiently suppresses p21 expression induced by Ad-p53–mediated p53 overexpression. Ad-p53 infection at MOIs of 10 and 100 efficiently induced p21 expression at 48 hours after infection in SaOS-2 cells (Supplementary Fig. S5). When SaOS-2 cells were infected with Ad-p53 at an MOI of 100 for 48 hours, pretransfection with *miR-93*, *miR-106b*, or both efficiently suppressed Ad-p53–induced p21 expression (Fig. 3D). Interestingly, both *miR-93*- and *miR-106b*–transfected SaOS-2 cells showed the 1.5-fold increased expression of cleaved PARP (C-PARP) in consistency with remarkable p21 downregulation when compared with those transfected with control miR. However, the expression level of C-PARP was not increased in the *miR-93*- or *miR-106b*–transfected SaOS-2 cells, although transfection with *miR-93* or *miR-106b* moderately decreased p21 expression. These results suggest that OBP-702 suppresses p21 expression through E1A-dependent upregulation of both E2F1-inducible *miR-93* and *miR-106b* and contributes to induction of apoptosis.

Increased induction of autophagy by OBP-702 when compared with OBP-301

Recently, we showed that oncolytic adenovirus OBP-301 mainly induces programmed cell death in association with autophagy rather than apoptosis in human tumor

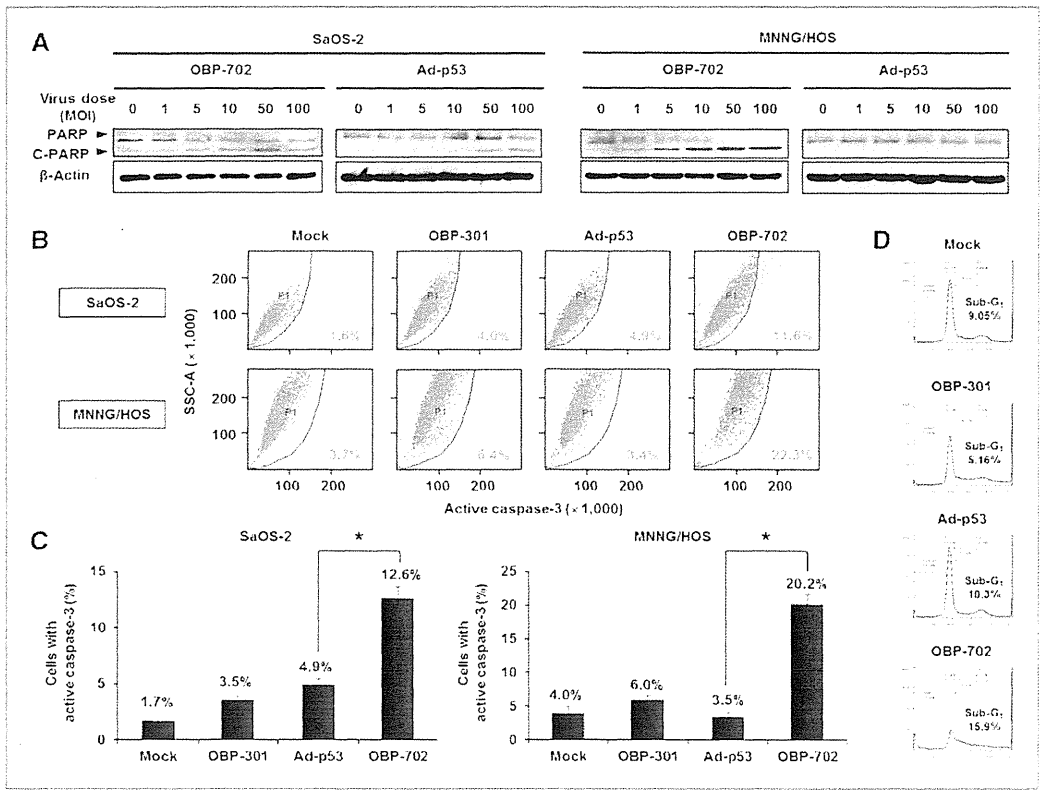

Figure 2. OBP-702 induces increased apoptosis when compared with OBP-301 or Ad-p53. A, OBP-301–resistant SaOS-2 and MNNG/HOS cells were infected with OBP-702 or Ad-p53 at the indicated MOIs for 72 hours. Cell lysates were subjected to Western blot analysis for the C-PARP and PARP. β-Actin was assayed as a loading control. B–D, SaOS-2 and MNNG/HOS cells were infected with OBP-702, OBP-301, or Ad-p53 at an MOI of 10 for 48 hours. Mock-infected cells were used as control. Caspase-3 activation was quantified using the flow cytometric analysis. Representative flow cytometric data are shown in B. The mean percentage of SaOS-2 cells and MNNG/HOS cells that express active caspase-3 was calculated on the basis of 3 independent experiments (C). The cell-cycle state was analyzed by flow cytometry in SaOS-2 cells after staining with propidium iodide. Representative cell-cycle data are shown (D). The percentage of sub-G_1 population was expressed in each graph. Bars, SD. Statistical significance was determined using Student *t* test. *, $P < 0.05$.

cells (31). Therefore, we next investigated whether OBP-702 induces more profound autophagy than does OBP-301. Western blot analysis revealed that OBP-702 infection showed increased autophagy, which was confirmed by conversion of LC3-I to LC3-II (increased ratio of LC3-II/LC3-I) and p62 downregulation, when compared with OBP-301 in MNNG/HOS cells (Fig. 4A). Moreover, the expression level of the p53-induced modulator of autophagy, DRAM (32), was decreased after OBP-301 infection, but its expression was maintained after OBP-702 infection (Fig. 4A). As p53-mediated p21 overexpression is known to inhibit both apoptosis and autophagy (17, 18), we further evaluated whether miR-mediated p21 suppression is involved in the enhancement of p53-mediated autophagy induction. Ad-p53–induced autophagy was enhanced by *miR-93-* and *miR-106b*–mediated p21 suppression (Fig. 4B). These results suggest that OBP-702 induces more profound autophagy than does OBP-301 and that this effect occurs via p53-mediated DRAM activation and miR-mediated p21 suppression.

Enhanced antitumor effect of OBP-702 in an orthotopic xenograft tumor model

Finally, to assess the *in vivo* antitumor effect of OBP-702, we used an orthotopic MNNG/HOS tumor xenograft model. OBP-702, OBP-301, Ad-p53, or PBS were intratumorally injected for 3 cycles every 2 days. OBP-702 administration significantly suppressed tumor growth when compared with OBP-301, Ad-p53, or PBS in an orthotopic MNNG/HOS tumor model (Fig. 5A and B). 3D-CT examination revealed that OBP-702–treated tumors had less bone destruction than did OBP-301- or Ad-p53–treated